Functional and evolutionary perspectives on gill structures of an obligate air-breathing, aquatic snail (#34352)

First revision

Guidance from your Editor

Please submit by **6 Jun 2019** for the benefit of the authors (and your $200 publishing discount).

Structure and Criteria
Please read the 'Structure and Criteria' page for general guidance.

Raw data check
Review the raw data. Download from the location described by the author.

Image check
Check that figures and images have not been inappropriately manipulated.

Privacy reminder: If uploading an annotated PDF, remove identifiable information to remain anonymous.

Files
Download and review all files from the materials page.

1 Tracked changes manuscript(s)
1 Rebuttal letter(s)
15 Figure file(s)
3 Table file(s)

Structure and Criteria

Structure your review

The review form is divided into 5 sections. Please consider these when composing your review:

1. **BASIC REPORTING**
2. **EXPERIMENTAL DESIGN**
3. **VALIDITY OF THE FINDINGS**
4. General comments
5. Confidential notes to the editor

You can also annotate this PDF and upload it as part of your review

When ready submit online.

Editorial Criteria

Use these criteria points to structure your review. The full detailed editorial criteria is on your guidance page.

BASIC REPORTING

- Clear, unambiguous, professional English language used throughout.
- Intro & background to show context. Literature well referenced & relevant.
- Structure conforms to PeerJ standards, discipline norm, or improved for clarity.
- Figures are relevant, high quality, well labelled & described.
- Raw data supplied (see PeerJ policy).

EXPERIMENTAL DESIGN

- Original primary research within Scope of the journal.
- Research question well defined, relevant & meaningful. It is stated how the research fills an identified knowledge gap.
- Rigorous investigation performed to a high technical & ethical standard.
- Methods described with sufficient detail & information to replicate.

VALIDITY OF THE FINDINGS

- Impact and novelty not assessed. Negative/inconclusive results accepted. *Meaningful* replication encouraged where rationale & benefit to literature is clearly stated.
- All underlying data have been provided; they are robust, statistically sound, & controlled.
- Speculation is welcome, but should be identified as such.
- Conclusions are well stated, linked to original research question & limited to supporting results.

Standout reviewing tips

The best reviewers use these techniques

Tip	*Example*
Support criticisms with evidence from the text or from other sources	*Smith et al (J of Methodology, 2005, V3, pp 123) have shown that the analysis you use in Lines 241-250 is not the most appropriate for this situation. Please explain why you used this method.*
Give specific suggestions on how to improve the manuscript	*Your introduction needs more detail. I suggest that you improve the description at lines 57- 86 to provide more justification for your study (specifically, you should expand upon the knowledge gap being filled).*
Comment on language and grammar issues	*The English language should be improved to ensure that an international audience can clearly understand your text. Some examples where the language could be improved include lines 23, 77, 121, 128 – the current phrasing makes comprehension difficult.*
Organize by importance of the issues, and number your points	*1. Your most important issue* *2. The next most important item* *3. …* *4. The least important points*
Please provide constructive criticism, and avoid personal opinions	*I thank you for providing the raw data, however your supplemental files need more descriptive metadata identifiers to be useful to future readers. Although your results are compelling, the data analysis should be improved in the following ways: AA, BB, CC*
Comment on strengths (as well as weaknesses) of the manuscript	*I commend the authors for their extensive data set, compiled over many years of detailed fieldwork. In addition, the manuscript is clearly written in professional, unambiguous language. If there is a weakness, it is in the statistical analysis (as I have noted above) which should be improved upon before Acceptance.*

Functional and evolutionary perspectives on gill structures of an obligate air-breathing, aquatic snail

Cristian Rodriguez [Equal first author, 1, 2, 3], **Guido I Prieto** [Equal first author, 3], **Israel A Vega** [Corresp., 1, 2, 3], **Alfredo Castro-Vazquez** [Corresp. 1, 2, 3]

[1] IHEM, CONICET, Universidad Nacional de Cuyo, Mendoza, Argentina

[2] Instituto de Fisiología, Facultad de Ciencias Médicas, Universidad Nacional de Cuyo, Mendoza, Argentina

[3] Departamento de Biología, Facultad de Ciencias Exactas y Naturales, Universidad Nacional de Cuyo, Mendoza, Argentina

Corresponding Authors: Israel A Vega, Alfredo Castro-Vazquez
Email address: israel.vega7@gmail.com, a.castrovazquez@gmail.com

Ampullariids are freshwater gastropods bearing a gill and a lung, thus showing different degrees of amphibiousness. In particular, *Pomacea canaliculata* (Caenogastropoda, Ampullariidae) is an obligate air-breather that relies mainly or solely on the lung for dwelling in poorly oxygenated water, for avoiding predators, while burying in the mud during aestivation, and for oviposition above water level. In this paper, we studied the morphological peculiarities of the gill in this species. We found (1) the gill and lung vasculature and innervation are intimately related, allowing alternation between water and air respiration; (2) the gill epithelium has features typical of a transporting rather than a respiratory epithelium; and (3) the gill has resident granulocytes within intraepithelial spaces that may serve a role for immune defence. Thus, the role in oxygen uptake may be less significant than the roles in ionic/osmotic regulation and immunity. Also, our results provide a morphological background to understand the dependence on aerial respiration of *P. canaliculata*. Finally, we consider these findings from a functional perspective in the light of the evolution of amphibiousness in the Ampullariidae, and discuss that master regulators may explain the phenotypic convergence of gill structures amongst this molluscan species and those in other phyla.

Functional and evolutionary perspectives on gill structures of an obligate air-breathing, aquatic snail

Cristian Rodriguez[1,2,3†], Guido I Prieto[3†], Israel A Vega[1,2,3*], Alfredo Castro-Vazquez[1,2,3*]

[1] IHEM, CONICET, Universidad Nacional de Cuyo, Mendoza, Argentina.
[2] Universidad Nacional de Cuyo, Facultad de Ciencias Médicas, Instituto de Fisiología, Mendoza, Argentina.
[3] Universidad Nacional de Cuyo, Facultad de Ciencias Exactas y Naturales, Departamento de Biología, Mendoza, Argentina.

[†]These authors contributed equally to this work.

* Corresponding Authors
Alfredo Castro-Vazquez
Centro Universitario, Casilla de Correo 33, 5500 Mendoza, Argentina
Email address: a.castrovazquez@gmail.com
Israel A. Vega
Centro Universitario, Casilla de Correo 33, 5500, Mendoza, Argentina
Email address: iavega.conicet@gmail.com

Abstract

Ampullariids are freshwater gastropods bearing a gill and a lung, thus showing different degrees of amphibiousness. In particular, *Pomacea canaliculata* (Caenogastropoda, Ampullariidae) is an obligate air-breather that relies mainly or solely on the lung for dwelling in poorly oxygenated water, for avoiding predators, while burying in the mud during aestivation, and for oviposition above water level. In this paper, we studied the morphological peculiarities of the gill in this species. We found (1) the gill and lung vasculature and innervation are intimately related, allowing alternation between water and air respiration; (2) the gill epithelium has features typical of a transporting rather than a respiratory epithelium; and (3) the gill has resident granulocytes within intraepithelial spaces that may serve a role for immune defence. Thus, the role in oxygen uptake may be less significant than the roles in ionic/osmotic regulation and immunity. Also, our results provide a morphological background to understand the dependence on aerial respiration of *P. canaliculata*. Finally, we consider these findings from a functional perspective in the light of the evolution of amphibiousness in the Ampullariidae, and discuss that master regulators may explain the phenotypic convergence of gill structures amongst this molluscan species and those in other phyla.

Introduction

Respiratory organs are identified as either gills or lungs, whether they are formed as protrusions or as invaginations of the respiratory mucosae. Gills are almost always used for aquatic respiration, while lungs are for aerial respiration, but in addition to respiration, these organs may also serve other functions (Maina 2000a; Maina 2002b).

In bimodal breathers (i.e. aquatic animals that have retained a gill while developing a respiratory organ for breathing air), the gill may partially lose the respiratory role while acquiring others. In such cases, the respiratory function is supplied mainly by the air-breathing organ. In bimodal crustaceans and fishes, for example, the dependence on water comes in grades, the lesser water-dependent species having well-developed lungs that take up oxygen from the air and reduced or modified gills for ionic/osmotic regulation and CO_2 excretion (Farrelly & Greenaway 1987; Graham et al. 2007; Hughes & Morgan 1973; Innes & Taylor 1986; Low et al. 1988).

Most gastropods are marine and bear ctenidial gills (Haszprunar 1988), but some have adapted to terrestrial and amphibious life by developing lungs as specialisations of the pallial cavity (Semper 1881). Lungs occur in the subclasses Neritimorpha, Caenogastropoda and Heterobranchia (sensu Bouchet et al. 2017), although differing substantially in structure (Lindberg & Ponder 2001). In the majority of lung-bearing gastropods, the pallial cavity itself has been modified as a lung (Lindberg & Ponder 2001). Therefore, in these cases, the pallial cavity and the lung are homologous structures (Ruthensteiner 1997). In turn, in the family Ampullariidae (Caenogastropoda), the lung is a sac with a single cavity that extends on the roof of the pallial cavity and thus is not homologous with the pallial cavity.

Ampullariids comprise bimodal breathers that have also retained a true gill (i.e. a ctenidium). As other bimodal breathers, ampullariids show different degrees of amphibiousness, being the genera *Afropomus*, *Saulea*, *Lanistes*, *Asolene*, *Felipponea*, and *Marisa* more water-dependent than *Pila* and *Pomacea* (Hayes et al. 2009a). Amongst the latter, *Pomacea canaliculata* (Lamarck, 1822) is an obligate air-breather (Seuffert & Martín 2010) that has a well-developed lung and a left nuchal lobe that is capable of being rolled into a siphon-like tube, and which uses as a snorkel to ventilate the lung while being submerged (Andrews 1965). Behavioural observations have shown that *P. canaliculata* relies mainly or solely on the lung for dwelling in poorly oxygenated waters, for avoiding predators (Ueshima & Yusa 2015), while burying in the mud during aestivation (d'Orbigny 1847; Giraud-Billoud et al. 2011; Giraud-Billoud et al. 2013; Hayes et al. 2015), and for oviposition above the water level (Hayes et al. 2009b). These facts make *P. canaliculata* (and the Ampullariidae in general) interesting models to investigate the suitability of respiratory organs, i.e. the gill and the lung, for the exchange of gases as well as the structural and functional integration of both organs. In a far-reaching perspective, such studies can help us understand the evolution of amphibiousness.

However, there is a paucity of data regarding the fine structure of caenogastropod gills. Previous studies have been limited to the hypertrophied ctenidia of hot vent caenogastropods (Provannidae; e.g., Endow & Ohta 1989; Stein et al. 1988; Windoffer & Giere 1997), which bear large quantities of endosymbiotic bacteria, but these studies have been aimed at elucidating the relationship between gill epithelial cells and their endosymbionts. In the Ampullariidae, the gill structure has been studied in *Pila globosa* (Swainson, 1822), *Marisa cornuarietis* (Linnaeus, 1758), and *P. canaliculata* (Andrews 1965; Lutfy & Demian 1965; Prashad 1925), but only at the ~~histological~~ level. In this paper, we present a thorough description of the gill of *P. canaliculata* at the anatomical (3D rendering of its blood system), ~~histological,~~ and ultrastructural levels. Surprisingly, gill structures have never been investigated in this respect with fine structural techniques before. Therefore, our findings are a significant contribution to the knowledge of gill structures of ampullariids and the extremely large group of caenogastropods in general. Also, we discuss the significance of our findings from a functional and evolutionary perspective.

Material and methods

Animals and culturing conditions

Animals (young adult males, 20 mm shell length) were obtained from the Rosedal strain of *P. canaliculata*, whose origin and culture conditions have been described several times elsewhere (e.g., Cueto et al. 2015; Rodriguez et al. 2018). Animals were immersed in water at 4°C for 20–30 minutes both for relaxation and minimizing pain, before careful shell cracking. Procedures for snail culture, sacrifice, and tissue sampling were approved by the Institutional Committee for the Care and Use of Laboratory Animals (Comité Institucional para el Cuidado y Uso de Animales de Laboratorio (CICUAL), Facultad de Ciencias Médicas, Universidad Nacional de Cuyo), Approval Protocol N° 55/2015.

Light and electron microscopy

The gills from six animals were dissected out, fixed in dilute Bouin's fluid (1:2), dehydrated in a graded ethanol series, cleared in xylene and embedded in a 1:1 paraffin–resin mixture (Histoplast®, Argentina). Sections (3–5 μm thick) were obtained and stained with Gill's haematoxylin and eosin. The stained sections were examined and photographed under a Nikon Eclipse 80i microscope using Nikon DS-Fi1-U3 camera and Nikon NIS-ELEMENT Image Software for image acquisition.

Additionally, the gill, lung and pericardium were dissected out as a single piece from two animals, and were used for 3D reconstruction of the gill's blood system and for descriptions of its innervation. For these purposes, the lung was collapsed before fixation in dilute Bouin's fluid, to reduce the size of the dissected sample~~, and then,~~ serial sections (10 μm thick) were stained with Gill's haematoxylin and eosin and photographed with a Nikon Digital Sight DS-5M camera on a Nikon Alphaphot-2 YS2 microscope.

Also, gill samples from six animals, each one including ~20 consecutive leaflets, were prepared for scanning electron microscopy. For this purpose, the samples were fixed in dilute Bouin's fluid and some of them were microdissected to show different aspects of the leaflets. Afterwards, they were dehydrated in an ethanol series, passed through acetone and then critical point dried, mounted on aluminium stubs, coated with gold, and examined with a Jeol/EO JSM-6490LV scanning electron microscope.

Furthermore, gill samples from six additional animals were fixed in Karnovsky's fluid (4% paraformaldehyde, 2.5% glutaraldehyde, dissolved in 0.1 M phosphate buffer, pH 7.4). One day later, tissues were washed thrice in phosphate buffer and transferred to 1% osmium tetroxide overnight. Afterwards, they were gradually dehydrated in a graded acetone series and finally embedded in Spurr's resin. Ultramicrotome sections (~200 nm) were stained with toluidine blue and covered with DPX medium (Sigma-Aldrich) for fine histology. Silver-grey, ultrathin sections of gill samples were mounted on copper grids and stained with uranyl acetate and lead citrate, and examined with a Zeiss EM 900 transmission electron microscope.

Computerised 3D rendering of the gill blood system

Digital images of every fifth section were aligned manually using Reconstruct, version 1.1.0.0 (Fiala 2005), downloaded from Synapse Web, Kristen M. Harris, PI (http://synapses.clm.utexas.edu). Then, the profile of identified structures (*objects*) were drawn with the mouse using the Trace tool. These *traces* were used for the 3D visualisation of object

structures. The 3D model was exported as a VRML 2.0 file and embedded in a PDF as described by Ruthensteiner & Heß (2008), using the 3D tool of Adobe Acrobat 9 Pro Extended software.

Results

General organisation of the gill and related pallial organs

The respiratory organs in the pallial complex are the gill and the lung. In addition, there are other organs that serve an accessory function, namely the siphon (=left nuchal lobe), the right nuchal lobe, and the pallial fold, which are depicted in Fig. 1A.

The gill extends from the left rear end of the mantle cavity (in the proximity of the pericardium and next to the ureter) to the right front side of the mantle cavity (close to the anus and the copulatory apparatus), and borders the posterior and right sides of the lung (Fig. 1A). The gill is formed by a single row of rather parallel leaflets (i.e. a ctenidial monopectinate condition) that hang from their bases in the roof of the mantle cavity, in which the main afferent and efferent vessels run (Fig. 1B). The gill leaflets have a rather triangular shape with free edges of unequal length (Supplemental Fig. S1). Based on their relative position with respect to the blood flow, the shorter free edge is the afferent border, and the longer is the efferent one. The basal border is anchored to the branchial base and therefore to the outer mantle.

The lung extends through most of the roof of the mantle cavity and communicates with the mantle cavity through the pneumostome, close to the underlying air-breathing siphon. The pallial fold is a mucosal ridge that extends on the floor of the mantle cavity. It originates at the left posterior end of the mantle cavity, close to the pericardium, and runs to the right until it crosses the prostate (or the vagina in females) and then takes a diagonal anteroposterior direction towards the proximity of the right nuchal lobe. A functionally significant narrow channel is delimited between this fold, the gill, and the rear wall of the mantle cavity. The right nuchal lobe appears in fixed specimens as a short mucosal triangular fold hanging from the right side of the neck (Fig. 1A). In living animals, however, it is a thin scoop-like structure, which may occlude partly or totally the excretory mantle opening.

Blood circulation in the gill

The 3D rendering of the blood system of the gill (Fig. 2A–C and Supplemental Fig. S2) shows the *afferent branchial vessel* collects blood from ureteral efferents, particularly the *efferent ureteral vessel* (=*efferent renal vein* in Andrews 1965). Additionally, other gill afferents come from the *rectal sinus* and *right pallial vessels* that drain blood from the visceral hump. These afferents join the *afferent branchial vessel*, which continues as the *afferent pulmonary vessel*. Blood from the *afferent branchial vessel* flows through the gill leaflets to the *efferent pulmobranchial vessel* and then to the heart auricle, or alternatively, to the *ventral afferent pulmonary vessel* that irrigates the right half of the lung floor, thus integrating branchial and pulmonary circulation.

The haemocoel within each gill leaflet (Fig. 2D–F and Supplemental Fig. S2) extends as a lamina interrupted by trabeculae connecting both lateral surfaces of the leaflet, and is identified here as the *laminar leaflet sinus*. However, there are also two rather continuous haemocoelic sinuses in each leaflet: a *marginal leaflet sinus* runs along the free border of each leaflet, while the other, namely the *basal leaflet sinus*, extends at the base of the gill as a short cut between the *afferent branchial vessel* and the *efferent pulmobranchial vessel*. These sinuses communicate extensively with the *laminar leaflet sinus*, which also connects with the *ventral afferent pulmonary vessel*.

Branchial nerves and their origins

Innervation of the gill of *P. canaliculata* comes from the *supraoesophageal ganglion* and an *accessory visceral ganglion*, which are diagrammatically shown in Fig. 3A.

Nerve branches of the *branchial nerve* arising from the *supraoesophageal ganglion* go through the lung roof (perhaps giving off neurites that innervate the lung roof) and end at the base of the gill leaflets (C. Rodriguez, G.I. Prieto, I.A. Vega & A. Castro-Vazquez, unpubl. data). Each gill leaflet, however, shows a nerve along its efferent border (Fig. 3B). These *leaflet nerves* presumably originate from branches of the *branchial nerve*.

The *accessory visceral ganglion* is located in the supraoesophageal portion of the visceral loop, close to the pericardium, and gives off a nerve longitudinally traversing the ureter and running along the base of the gill, next to the *afferent branchial vessel* (Fig. 3C). The latter nerve has not been referred for *P. canaliculata* (or for any other ampullariid) and it is here referred to as the *branchial base nerve*, which accompanies the *afferent branchial vessel*.

Also, neurite bundles arising from the *copulatory ganglion* are likely to join the *branchial base nerve* through its anterior end (Fig. 3D), at least in male animals. The *copulatory ganglion* lies close to the anterior end of the gill, in the proximity of the anus and the copulatory apparatus.

The gill leaflets and their regions

Four regions may be distinguished in each leaflet that are characterised by different epithelia (Figs. 4A and 5A). Under scanning electron microscopy, region I appears covered by microvillar cells and interspersed ciliary cells (Fig. 5A), whereas regions III and IV are respectively covered with cells bearing either long (Fig. 5B) or short cilia (Fig. 5C). Region II differs from region I in that it shows no ciliary cells (Fig. 4D–E). A summary of data is provided in Table 1.

The *laminar leaflet sinus* occupies the central space of each leaflet and is bordered by a thin fibromuscular layer, which underlies the epithelium (Fig. 4). The sinus is traversed by trabeculae (Fig. 4B–C), which in regions I and II are thinner than in region III (Fig. 4D–E).

The *leaflet nerve* (Fig. 6A) runs along the efferent *marginal leaflet sinus* and it is partly sheathed in a bundle of longitudinal muscle fibres (U-shaped in sections). This bundle is referred to as the supporting rod (Fig. 6B). At closer examination, the *leaflet nerve* is formed by tightly packed neurites and some glial processes (Fig. 6C–D), whereas the supporting rod is formed by large muscle fibres ~~immersed in~~ a dense collagen matrix (Fig. 6E).

Epithelial cell types

The epithelium varies widely in the different regions of each leaflet (data is summarised in Table 2). In region I, it is columnar or low columnar (20–40 µm), and it is mainly composed of either clear or dark microvillar, mitochondria-rich cells, hereafter referred to as α-cells and β-cells, respectively (Fig. 7). Besides that, there are also interspersed ciliary cells, and a few secretory cells. These cells (identified as C1, S1 and S2 cells, respectively) will be described for region IV, where they are more abundant.

Alpha-cells are characterised by euchromatic nuclei and conspicuous nucleoli. The cytoplasm contains numerous long mitochondria with well-defined cristae and glycogen deposits (Fig. 8A–C). Apically, these cells show few and rather short microvilli, and underlying membrane-bound bundles of electron-dense filaments/tubules. There is also a well-developed endomembrane vesicular system, as well as multivesicular (Fig. 8B) and multilamellar bodies (Fig. 8C).

Contrasting with α-cells, β-cells bear heterochromatic nuclei and a cytoplasm with numerous and tightly packed mitochondria (Fig. 8D–F). The surface area of the apical domain is increased by numerous and ramified microvilli (see Fig. 5A). An apical narrow band of homogeneous cytoplasm is seen below the microvilli, together with the apical ends of an extensive tubular system, which extends to the underlying mitochondrial conglomerate (Fig. 8E). Multivesicular bodies as well as presumptively degenerative bodies, such as myeloid bodies and fibrogranular material, are also abundant in the perinuclear region of these cells (Fig. 8F). Alpha-cells and β-cells alternate in approximately equal numbers. Numerous granulocytes lay inside epithelial intercellular spaces all along region I (Fig. 9), although they may also occur in other regions (see next Section).

A single cell type constitutes the epithelium in region III, which rests on a well-defined and electron-dense basal lamina (Fig. 10). It consists of cells with slender nuclei, very long cilia and short microvilli (C2 cells), and whose basolateral plasma membranes often enclose extensive and apparently dynamic intercellular spaces. The cytoplasm contains abundant rough endoplasmic reticulum and glycogen deposits (Fig. 10A–B). Transverse sections of cilia (Fig. 10C) show the typical 9+2 microtubule arrangement as well as membrane blebs (Fig. 10C, arrows). As α-cells, these cells have membrane-bound bundles of electron-dense filaments/tubules in the subapical region (Fig. 10D).

The epithelium in region IV rests on a well-defined and electron-dense basal lamina and exhibits the same cell types as epithelium in region I, except for β-cells (Fig. 11A). However, ciliary C1 cells are the most abundant cell type here. They are characterised by a heterochromatic nucleus and an electron-dense cytoplasm that contains large dense-cored granules and glycogen deposits (Fig. 11B). The subapical region is similar to those of α-cells, but apically there are finger-like microvilli and short cilia (Fig. 11B). Secretory S1 cells are mucous cells with merging granules containing an electron-dense mesh above the nucleus (Fig. 11C), and granules with a looser electron-dense mesh in the apical domain (Fig. 11D). These granules would correspond to the densely and loosely metachromatic accumulations seen in toluidine blue preparations (see Figs. 4E and 6A). On the other hand, secretory S2 cells have their cytoplasm almost filled with granules with a low electron-dense core (Fig. 11E), which are orthochromatic in toluidine blue preparations (Figs. 4E and 6A).

Epithelium in region II exhibits α-cells, and abundant S1 and S2 cells (Fig. 4). The epithelia in regions III and IV are those directly exposed to the incoming water current that flows over the gill, and both the long and short cilia may contribute to the water movement.

Apical intercellular junctions and the basolateral domain of epithelial cells

All epithelia examined showed two types of cellular junctions in an orderly fashion. Apical adherent junctions (also called *zonula adhaerens* or ‘desmosome belt’; Fig. 12A) are followed by septate junctions (Fig. 12B), which are often interrupted by intercellular canaliculi (Fig. 12A–B). Rather frequently, the canaliculi contain a globular, unidentified material (Fig. 12A). Below the septate junctions, the adjacent plasma membranes are separated by larger spaces, which increase in size towards the basal domain (Fig. 12C).

The basolateral domain of epithelial cells in all regions of a leaflet is a labyrinth of intermingled thin extensions that project towards the underlying connective tissue. There are conspicuous spaces between epithelial cells, which are frequently occupied by granulocytes (Fig. 9). Small neurite bundles, with or without accompanying glial cells, are also found in the intercellular spaces, thus providing direct intraepithelial innervation (Fig. 9A, arrows). A

collagen matrix and sparse muscle fibres form the underlying connective tissue, which delimits the leaflet haemocoel. Neurite bundles accompanied by glial cells are frequently found in this tissue (see Fig. 9A), and these will be further described in the next Section.

A notable feature of this epithelium is the occurrence of granulocytes, with eccentric nuclei and conspicuous nucleoli, electron-dense granules, and areas of glycogen deposits. Granulocytes are often fully enclosed into expanded intercellular spaces (Fig. 9A–B), but sometimes, discontinuities in the mesh of basal projections of epithelial cells are found (Fig. 9C). These discontinuities connect the intercellular spaces directly with the basal lamina, which is evident because of its well-delimited *lamina densa* with interspersed electron-dense thickenings (Fig. 9C, arrowheads).

Fibromuscular tissue and fine innervation

Underlying the basal lamina there are muscle cells embedded in a collagen matrix (Fig. 13A). These muscle cells show myofibrils and scarce mitochondria. The cell surface shows numerous electron-dense anchoring junctions composed of an external brush-like plaque and an internal amorphous but electron-dense layer (Fig. 13B). The fibrils of the brush-like plaques are often continuous with those of other cell plaques or with thickenings of the *lamina densa* (Fig. 13A–B, arrowheads). These peculiar structures lie over clear cytoplasmic areas, which are traversed by thin cytoskeletal fibres.

Numerous neurite bundles that traverse the connective tissue and sometimes go into the epithelial intercellular spaces provide leaflet innervation. Neurites form bundles that are flanked by glial cell processes (Fig. 13C). Glial cells, or less frequently, uncovered neurites are in contact with muscle cells. Glial cells have rounded electron-dense, membrane-bound, granules of two different sizes (either ~400 nm or ~100 nm wide). Neurites have an electron-lucent axoplasm with neurofilaments. Fibre enlargements (presumptive nerve endings) contain ~80 nm wide granules of variable electron density and ~50 nm wide clear vesicles (Fig. 13C).

Discussion

Comparative aspects of the gill leaflets and supporting structures

Most gastropod ctenidia are composed of triangular leaflets (Lindberg & Ponder 2001) that commonly have four ciliary fields, namely the lateral, frontal, abfrontal, and terminal. Lateral cilia are placed in two rows alongside the efferent border of the leaflet and provide ventilation, while the others cover the free edges of the leaflet and are engaged in cleansing (Lindberg & Ponder 2001; Yonge 1947). The gill leaflets of *Pomacea canaliculata* are rather triangular and have well-developed lateral and frontal ciliary fields, which are here referred to as regions III and IV respectively (Fig. 4), but have not abfrontal or terminal cilia. The identity and disposition of the ciliary fields, as well as the rather small variation in shape and size of the leaflets along the gill in this species (Supplemental Fig. S1), are similar to those of *Marisa cornuarietis* (Demian 1965; Lutfy & Demian 1965).

An efficient respiratory organ requires a both large and thin surface area. This respiratory surface should be fully exposed to the external medium to allow gas exchange (Maina & West 2005). Therefore, some mechanical rigidity to support a deployed gill is indispensable to permit an adequate gas exchange. Structures that support the weight of gills have been found in different taxa, such as the cartilaginous or bony supporting rods (gill rays), the interbranchial septa, and the ‘pillar cells’ in fishes (Evans et al. 2005), the cuticle, the intralamellar septa, and the pillar cells in crustaceans (e.g., Farrelly & Greenaway 1987; Farrelly & Greenaway 1992), and the

'supporting skeletal rods' and 'trabecular cells' in molluscs (Nakao 1975; Ridewood 1903; Yonge 1947).

Skeletal rods may be accompanied by a nerve along the efferent (in gastropods and bivalves) or afferent (in cephalopods) border of gill leaflets (Yonge 1947). According to Haszprunar (1988), skeletal rods have arisen several times in the evolution of molluscs in general, and twice amongst gastropods, namely in the Vetigastropoda and in the Ampullariidae (Caenogastropoda). Hyman (1967) had already referred the rod for the vetigastropod families Haliotidae, Trochidae, and Fissurellidae. Furthermore, Wanichanon et al. (2004) have reported the rod of *Haliotis asinina* (Haliotidae) as a 'chitinous' structure accompanied by a muscle bundle, and also Eertman (1996) mentioned the existence of a rod in the gill leaflets of *Austrocochlea constricta* (Trochidae), but he did not study its ultrastructure.

Although a 'skeletal rod' of the Ampullariidae has been mentioned several times (Berthold 1991; Haszprunar 1988; Ponder & Lindberg 1997; Salvini-Plawen & Haszprunar 1987), no information on its microstructure was given in those papers. In *P. canaliculata*, we found that a supporting rod occurs in the efferent margin of each gill leaflet. It is U-shaped in sections and made of large muscle fibres embedded in a collagen matrix (see Fig. 13), i.e. a fibromuscular contractile structure. Thus, it is not made of 'chitin', as in *H. asinina* (Wanichanon et al. 2004), or of merely collagen (Hyman 1967). It accompanies the *leaflet nerve* and the *marginal leaflet sinus*. It is worth noting that likely homologous muscular structures occur in the ampullariids *M. cornuarietis* (Lutfy & Demian 1965) and in *Pila globosa* (Prashad 1925). However, neither Lutfy & Demian (1965) nor Prashad (1925) referred the existence of a *leaflet nerve*. Considering that the three genera are closely related and that these authors used only light microscopy techniques, which are not best suited to recognise nervous tissue, they probably overlooked the *leaflet nerve*. Besides that, the homology of the muscular structures of these ampullariids with the skeletal/supporting rods of other gastropods remains as an unresolved issue. The muscular supporting rod would keep the gill leaflets deployed thus exposing the efferent margins to the water current flowing from left to right through the mantle cavity.

Trabecular cells are common structures in the molluscan gills, whether they are ctenidia (Gregory et al. 1996; Le Pennec et al. 1988; Manganaro et al. 2012; Nuwayhid et al. 1978) or secondary gills (De Villiers & Hodgson 1987; Jonas 1986). Trabeculae had been previously observed in ampullariids but were mistakenly considered as septa delimiting parallel blood sinuses (Andrews 1965; Lutfy & Demian 1965; Prashad 1925; Ranjah 1942).

Nakao (1975) described in detail the trabecular cells of the bivalve *Anodonta woodiana*. They are modified muscular cells with a cytoplasm almost filled with myofibrils, scarce peripheral organelles, and anchoring junctions. The modified muscular cells underlying the basal lamina in *P. canaliculata* (see Fig. 13A–B) show similar characteristics, and thus may correspond to the anchoring part of the trabeculae shown in Figs. 4 and 5C.

The gill as a respiratory organ

The 3D rendering of the blood system of the gill in *P. canaliculata* suggests that the general pattern of branchial blood circulation is similar to that described by Andrews (1965); although, there is a major difference that is worth mentioning (other differences can be found in Supplemental Table S1). The gill leaflets of *P. canaliculata* have a single laminar sinus interrupted by trabeculae and bounded by continuous sinuses at the leaflet borders and base, but with no transverse sinuses as interpreted by Andrews (1965) for this species, or by Lutfy & Demian (1965) for *M. cornuarietis*. This laminar arrangement implies a slow sheet-flow of

blood, which likely facilitates the exchange of respiratory gases (Maina 2000b; Maina 2002a) and, perhaps more importantly, of ions. Moreover, this 'sheet-flow design' is in agreement with that found in other molluscan, crustacean, and fish gills (e.g., Booth 1978; Knight & Knight 1986; Maina 1990). According to Andrews (1965), ciliary beating should conduct water between the gill leaflets towards a narrow channel bordered by the gill and the pallial fold. An exhalant water stream flows along the course of this channel, thus expelling urine and faeces (Andrews 1965). In this way, a countercurrent mechanism would occur between blood flowing through the leaflets and water flowing between them, facilitating the O_2 extraction from water (see Fig. 2F).

However, in spite of having a countercurrent mechanism for O_2 extraction, the gas exchange should be hindered by the thickness of the gill epithelium (>20 μm), according to Fick's first law of diffusion (Maina & West 2005). Also, the large number of mitochondria found in epithelial cells (see Figs. 6 and 7) indicates a high oxygen consumption, but this finding contradicts the idea that a respiratory tissue barrier must consume a minimal amount of the oxygen it extracts from the external medium (Maina 2000b). Indeed, a high oxygen consumption rate would be required for ion pumping against concentration gradients, which likely occurs in the gill epithelium. It should be considered, however, that a decrease in septate junctions' length –as occurs in leaflet region III– may shorten the distance between the external and internal media for the passage of molecules via the paracellular pathway (Yu 2017). It is therefore expected that some downhill diffusion of gases followed this route, which requires no energy expenditure. However, the gill CO_2 excretion would be higher than the O_2 uptake, because of the higher solubility of CO_2 in water. This is true, indeed, for many freshwater bimodal-breathing fishes (e.g., Evans et al. 2005) and crustaceans (e.g., Innes & Taylor 1986), in which CO_2 excretion occurs mainly through their gills, and O_2 uptake occurs mainly through their lungs.

Thus, in the gill leaflets of *P. canaliculata*, deoxygenated blood coming from the *afferent branchial vessel* would reach the *basal* and *marginal leaflet sinuses* and would distribute through the *laminar leaflet sinus*, where incomplete oxygenation should happen (Fig. 2F). In this way, partially oxygenated blood would converge either to the *efferent pulmobranchial vessel* or the *ventral afferent pulmonary vessel*, as shown in Fig. 2F. The fact that partially oxygenated blood went directly to the lung floor would prove to be useful to complete the O_2 uptake when the animal is submerged, because the gill might be insufficient to do that. Moreover, when on land, the collapse of leaflets and their laminar sinuses would force blood to follow the *basal* or *marginal sinuses* converging in the *ventral afferent pulmonary vessel* (Fig. 2F). In this way, there would be a shunt to the lung circulation, where oxygenation should reach its maximum (Maina 1990).

Alternatively, the gill may function as a ventilator, generating the left-to-right current that exposes water to the wall of the pallial cavity, where some gas exchange might occur, as suggested by Haszprunar (1992). Nonetheless, both the branchial and pallial surfaces together are still insufficient for respiration in *P. canaliculata*, because this species still needs to ventilate the lung through its siphon for an adequate oxygen supply (Seuffert & Martín 2010). Indeed, Seuffert & Martín (2010) showed that *P. canaliculata*'s microdistribution in the field is mostly restricted to 2–4 m from the nearest emergent substratum, and that impeding aerial respiration negatively affected its survivorship in aquaria.

The gill as an ionic/osmotic regulator

P. canaliculata is a hyperosmotic and hyperionic regulator and, like in many other freshwater animals, its gill may be involved in this regulation. Indeed, the gill of *P. canaliculata* has a high

ion-ATPase activity, which suggests it is a site of ion uptake from the surrounding water, while its ureter would be a site of ion reabsorption from the primary urine (Taylor & Andrews 1987).

As discussed above, the gill epithelium of *P. canaliculata* (Fig. 4) is characterised by tall columnar cells (>20 μm) with apical specialisations, numerous mitochondria, and basolateral infoldings of the plasma membrane that enclose broad and presumably dynamic intercellular spaces. Additionally, these highly polarised cells have well-developed endomembrane systems and glycogen deposits (see Figs. 6 and 7). In contrast, the gill epithelium of *M. cornuarietis* is lower (~10 μm) than that of *P. canaliculata*, and has no intercellular spaces (Lutfy & Demian 1965). It should be kept in mind that this species is more dependent on water than *P. canaliculata* (e.g., it lays gelatinous eggs underwater (e.g., it lays gelatinous eggs underwater; Hayes et al. 2009a), and thus relies mainly on its gill for respiration.

There are two main morphological types of presumptive ion-transporting cells in *P. canaliculata*, which may be equivalent to the α and β mitochondria-rich cells found in freshwater teleost fishes (for a review, see Evans et al. 2005; Wilson & Laurent 2002) and to the 'fibrillar' and 'tubulovesicular' types found in amphibians (Lewinson et al. 1987). Both α- and β-cells of *P. canaliculata* are indeed mitochondria-rich cells. Like those of fishes, α-cells have an electron-lucent cytoplasm, an apical membrane slightly concave with few and short apical specialisations, and a well-developed subapical vesicular system (Figs. 6 and 7A). This cell type also resembles the amphibian 'fibrillar cells' because of its membrane-bound bundles of electron-dense filaments/tubules (Fig. 7B). On the other hand, β-cells have an electron-dense cytoplasm and complex apical specialisations of the plasma membrane (Figs. 6 and 7D), as fish β-cells do. They also have a well-developed tubulovesicular system that almost fills the cytoplasm between mitochondria (Fig. 7E), in close resemblance to the 'tubulovesicular' cell type of amphibians (Lewinson et al. 1987). It should be noted that the highlighted similarities between fish, amphibian and *P. canaliculata*'s mitochondria-rich cell types suggest some similar regulatory mechanisms.

Thus, the features found in the gill epithelium of *P. canaliculata* contrast with those of the gill respiratory epithelia found in some other molluscan (e.g., Fischer et al. 1990; Gregory et al. 1996; Le Pennec et al. 1988; Manganaro et al. 2012; Nuwayhid et al. 1978) and non-molluscan taxa (e.g., Evans et al. 2005; Luquet et al. 2002) that are more dependent on water breathing, and which show cubic or squamous cells, with low nuclear/cytoplasmic ratios and a low content of mitochondria and other organelles. In turn, the gill structures found in *P. canaliculata* are more similar to those of transporting epithelia (Berridge & Oschman 2012), such as those of the vertebrate small intestine (e.g., Flik & Verbost 1993), gallbladder (e.g., Housset et al. 2016), and renal tubules (e.g., Yu 2017), and of the ionic/osmotic regulatory epithelia in the gills of crustaceans (e.g., Luquet et al. 2002; McNamara & Faria 2012) and fishes (e.g., McDonald et al. 1991). Taken together, these features may determine *P. canaliculata* to be an obligate air-breathing species, whose gill structures seem better suited for ionic/osmotic regulation than for O_2 uptake.

The gill as an immune barrier

In general, integumentary structures are the first barrier to microbial intruders, and as such, the gill is one of these structures preventing their access from the mantle cavity. In fact, *P. canaliculata* must also cope with the diverse symbiotic organisms that frequently dwell in the mantle cavity (Vega et al. 2006). Mucus secretion and water currents may be unfavourable for the settling of many organisms (Vega et al. 2006). Abundant mucus is found covering the gill

epithelium, which is likely secreted by the large number of secretory cells that occur in regions II and IV (Figs. 4 and 10). These cells are of two types, S1 and S2, that may correspond to the 'mucous' and 'gland' cell types in *M. cornuarietis*, respectively (Lutfy & Demian 1965).

However, the gill is also a potential barrier because of its position in the circulation, as are the kidney and lung in *P. canaliculata* (Rodriguez et al. 2018). Indeed, most blood coming from the cephalopodal mass and the visceral hump has to pass through the gill before reaching the heart to re-enter the general circulation. Thus, the gill itself, beyond its role as part of the integumentary barrier, may also function as a filter for blood-borne microorganisms.

The conspicuous occurrence of granulocytes amongst epithelial intercellular spaces (Figs. 4 and 8) suggests these cells would serve in immune surveillance in this organ. Granulocytes are also frequent in the gill of *M. cornuarietis*, but they appear subepithelial in the drawings of Lutfy & Demian (1965) rather than intraepithelial. The occurrence of immunocompetent cells within epithelial intercellular spaces is a widespread feature amongst the gills of bivalves (e.g., de Oliveira David et al. 2008; Gregory et al. 1996) and fishes (e.g., Hughes & Morgan 1973). The granulocytes found in the gill were larger than those found in the general circulation of *P. canaliculata* and, in spite of being the less frequent cell type in the circulation (see Cueto et al. 2015), the intercellular spaces had only granulocytes within them.

There is evidence of a kind of 'compound exocytosis' (Pickett & Edwardson 2006) leading to granulocyte degranulation in *P. canaliculata* (Cueto et al. 2015). Granulocyte degranulation in bivalves (e.g., Ciacci et al. 2009; Cheng et al. 1975; Foley & Cheng 1977; Mohandas et al. 1985; Rebelo et al. 2013) has been related to the release of lysozyme and other hydrolytic enzymes that may kill bacteria and fungi, and Ottaviani (1991) has reported lysozyme from haemocytes of a gastropod. Therefore, it is likely that granulocytes occurring in the intercellular spaces of the gill epithelium are there serving a defensive role against intruders in *P. canaliculata*.

Nervous control of the gill

The gill is mainly innervated from the *supraoesophageal ganglion* and the *accessory visceral ganglion* found in *P. canaliculata* (see Fig. 3A), which are part of the ganglionar visceral loop (Chase 2002) that also includes the suboesophageal and the visceral ganglia (Berthold 1991; Hylton Scott 1957). The origin of the gill innervation in the *supraoesophageal* and *accessory visceral* ganglia supports the view of the adult's gill as the post-torsional left gill (Lindberg & Sigwart 2015), but which has been displaced to the right by the development of the lung (Koch et al. 2009). The *branchial nerve* also innervates the osphradium and the muscular region of the lung that surrounds the pneumostome (C. Rodriguez, G.I. Prieto, I.A. Vega & A. Castro-Vazquez, unpubl. data). The osphradium has been shown to sense ionic or O_2/CO_2 levels in water, amongst other chemosensory functions in several gastropods (Lindberg & Sigwart 2015). It also may be involved in the switch between the behavioural modes of branchial and lung respiration (C. Rodriguez, G.I. Prieto, I.A. Vega & A. Castro-Vazquez, unpubl. data), and in the regulation of the gill ionic/osmotic functions in *P. canaliculata*.

We have not found any neuroepithelial cells similar to those found in fish gills (Bailly et al. 1992; Dunel-Erb et al. 1982; Jonz & Nurse 2003). The neurite supply to the gill leaflets is rich and spread in the connective tissue, the laminar sinus cells, and the epithelial basolateral domain (see Fig. 3), as has been described in the gill filaments of *Anodonta* (Nakao 1975) and in the gill leaflets of many fishes (e.g., Jonz & Zaccone 2009). It also includes glial cell processes (Fig. 12C) similar to those referred by Nicaise (1973) in heterobranchs.

The sensory information coming from the osphradium and/or the gill epithelium may be integrated in the visceral loop and may trigger different responses through efferent pathways. For example, controlling the state of the intercellular spaces could either increase or decrease the epithelium permeability, thus regulating respiratory or ionic/osmotic functions, as there has been described in fish gills (e.g., Jonz & Nurse 2006). Efferent pathways may also be involved in the regulation of vascular resistance through the gill leaflets by altering the stretching of trabecular cells, as has been proposed for bivalves (Nakao 1975) and as it occurs in pillar cells of fish gills (Jonz & Zaccone 2009). Indeed, numerous neurites were often found in close contact with these modified muscle cells (see Fig. 12). Finally, other motor innervation would involve that associated with the muscular supporting rod (see Fig. 6).

The evolution of amphibiousness: the family Ampullariidae as a case study

The family Ampullariidae has been proposed as a model for evolutionary biology because of its long evolutionary history that traces back to the Jurassic (~160 million years ago), wide geographic distribution (through Africa, Asia, and the Americas), and high diversity (~120 currently valid species) (Hayes et al. 2009a). These characteristics, along with the different degrees of air dependence ampullariids show, make this family an interesting model to study the evolution of amphibiousness (Hayes et al., 2015). Important advances have been made in elucidating the evolution of traits related to amphibiousness in Ampullariidae. In particular, the evolution of aerial oviposition has received considerable attention (e.g., Hayes et al. 2009a; Ip et al. 2019; Mu et al. 2017; Sun et al. 2019). However, a comparative study on the morphology, function, and development of the respiratory organs amongst the Ampullariidae is still lacking.

As mentioned above, the development of a lung has allowed a shift in the biological role of the gill to the detriment of its capacity for oxygen uptake in bimodal-breathing crustaceans and fishes. Our results suggest this may also be the case amongst the Ampullariidae and encourage the search for similar patterns through the comparison of the respiratory organs, and their relative functions, between ampullariid species with different degrees of air dependence.

Finally, it is worth emphasising the convergence of gill structures of *P. canaliculata* with those in phylogenetically distant taxa, such as arthropods (e.g., Farrelly & Greenaway 1987; Luquet et al. 2002; Maina 1990) and fishes (e.g., Evans et al. 2005; Laurent & Dunel 1980; Low et al. 1988; McDonald et al. 1991). Indeed, these may be cases of phenotypic convergence in which similar genetic mechanisms, such as the existence of conserved master regulators, can lead to convergence in form and function in independent and often distant lineages (Stern 2013). The existence of master regulators, such as the Hox and ParaHox genes, has been shown in ampullariids (Sun et al. 2019) and in representatives of other classes of molluscs (De Oliveira et al. 2016). Future studies may be aimed at elucidating whether conserved master regulators are involved in the development of similar structures in the gill of *P. canaliculata*.

Conclusions

1. We have confirmed interpretations of preceding authors regarding the vasculature and innervation of the gill of *P. canaliculata* and their implications. Namely, (a) that the gill vasculature is connected in series with that of the lung, in such a way that blood may complete oxygenation in the latter organ, and (b) that the origin of the gill innervation in the main and accessory supraoesophageal ganglia supports the view of the adult's gill as the post-torsional left gill, but which has been displaced to the right by the development of the lung.

2. When the animal is under water, the gill surface potentially available for gas exchange is large, but is covered by a rather thick epithelium (>20 μm), with no cubic or squamous cells as in the gills of crustaceans and fishes. Ultrastructural evidence suggests that the only structures that perhaps facilitate oxygen uptake would be those involved in the paracellular pathway.
3. Also, in case the branchial leaflets collapse when the animal is out of the water, blood may bypass the leaflets and go directly to the lung through a shunt formed between the *basal branchial sinuses* and the *ventral afferent pulmonary vessel*.
4. The leaflet architecture is uniform throughout the whole gill, i.e. there is not a respiratory and ionic regionalisation of the gill as there occurs in other taxa (e.g., crustaceans). However, four regions may be recognised within each leaflet, each presumably associated with specific functions: region I with ionic/osmotic regulation, regions II and IV with mucous secretion, regions III and IV with water circulation, and region III to gas exchange through the paracellular pathway.
5. Our findings showed that the gill epithelium has features of a transporting epithelium rather than a respiratory one. Specifically, the branchial epithelium has (1) developed apical specialisations and basolateral infoldings, (2) occluding junctions, (3) extensive, and likely dynamic, intercellular spaces, (4) a high density of mitochondria, and (5) an underlying rich nerve supply. Altogether, these features suggest the gill in *P. canaliculata* would be more suitable for ionic/osmotic regulation than for oxygen uptake, which partly explain why *P. canaliculata* is an obligate air-breathing species.
6. The gill may function as an immune barrier by secreting mucus to prevent the access of intruders from the mantle cavity, but also to prevent the spread of blood-borne microorganisms, in which granulocytes may participate.

Acknowledgements

The authors appreciate the generous help of Elisa Bocanegra, Sergio A. Carminati, Norberto F. Domizio, Mabel Fóscolo, María Silvina Lassa, and María Paula López.

References

Andrews EB. 1965. The functional anatomy of the mantle cavity, kidney and blood system of some pilid gastropods (Prosobranchia). *Journal of Zoology* 146:70-94.

Bailly Y, Dunel-Erb S, and Laurent P. 1992. The neuroepithelial cells of the fish gill filament: Indolamine-immunocytochemistry and innervation. *The Anatomical Record* 233:143-161.

Berridge MJ, and Oschman JL. 2012. *Transporting epithelia*: Elsevier.

Berthold T. 1991. Vergleichende Anatomie, Phylogenie und historische Biogeographie der Ampullariidae (Mollusca, Gastropoda). *Abhandlungen des Naturwissenschaftlichen Vereins in Hamburg* 29:1-257.

Booth JH. 1978. The distribution of blood flow in the gills of fish: application of a new technique to rainbow trout (*Salmo gairdneri*). *Journal of Experimental Biology* 73:119-129.

Bouchet P, Rocroi J-P, Hausdorf B, Kaim A, Kano Y, Nützel A, Parkhaev P, Schrödl M, and Strong EE. 2017. Revised classification, nomenclator and typification of gastropod and monoplacophoran families. *Malacologia* 61:1-527.

Ciacci C, Citterio B, Betti M, Canonico B, Roch P, and Canesi L. 2009. Functional differential immune responses of *Mytilus galloprovincialis* to bacterial challenge. *Comparative Biochemistry and Physiology Part B: Biochemistry and Molecular Biology* 153:365-371.

Cueto JA, Rodriguez C, Vega IA, and Castro-Vazquez A. 2015. Immune defenses of the invasive apple snail *Pomacea canaliculata* (Caenogastropoda, Ampullariidae): Phagocytic hemocytes in the circulation and the kidney. *PLoS ONE* 10:e0123964. 10.1371/journal.pone.0123964

Chase R. 2002. *Behavior and its neural control in gastropod molluscs.* Oxford: Oxford University Press.

Cheng TC, Rodrick GE, Foley DA, and Koehler SA. 1975. Release of lysozyme from hemolymph cells of *Mercenaria mercenaria* during phagocytosis. *Journal of Invertebrate Pathology* 25:261-265.

d'Orbigny A. 1847. Voyage dans l'Amérique Méridionale. Paris: C.P. Bertrand. p 711.

De Oliveira A, Wollesen T, Kristof A, Scherholz M, Redl E, Todt C, Bleidorn C, and Wanninger A. 2016. Comparative transcriptomics enlarges the toolkit of known developmental genes in mollusks. *BMC Genomics* 17:905.

de Oliveira David JA, Salaroli RB, and Fontanetti CS. 2008. Fine structure of *Mytella falcata* (Bivalvia) gill filaments. *Micron* 39:329-336.

De Villiers C, and Hodgson A. 1987. The structure of the secondary gills of *Siphonaria capensis* (Gastropoda: Pulmonata). *Journal of Molluscan Studies* 53:129-138.

Demian ES. 1965. The respiratory system and the mechanism of respiration in *Marisa cornuarietis* (L.). *Arkiv för Zoologi* 17:539-560.

Dunel-Erb S, Bailly Y, and Laurent P. 1982. Neuroepithelial cells in fish gill primary lamellae. *Journal of Applied Physiology* 53:1342-1353.

Eertman RHM. 1996. Comparative study on gill morphology of gastropods from Moreton Bay, Queensland. *Molluscan Research* 17:3-20.

Endow K, and Ohta S. 1989. The symbiotic relationship between bacteria and a mesogastropod snail, *Alviniconcha hessleri*, collected from hydrothermal vents of the Mariana Back-Arc Basin. *Bulletin of Japanese Society of Microbial Ecology* 3:73-82.

Evans DH, Piermarini PM, and Choe KP. 2005. The multifunctional fish gill: dominant site of gas exchange, osmoregulation, acid-base regulation, and excretion of nitrogenous waste. *Physiological Reviews* 85:97-177.

Farrelly C, and Greenaway P. 1987. The morphology and vasculature of the lungs and gills of the soldier crab, *Mictyris longicarpus*. *Journal of Morphology* 193:285-304.

Farrelly CA, and Greenaway P. 1992. Morphology and ultrastructure of the gills of terrestrial crabs (Crustacea, Gecarcinidae and Grapsidae): Adaptations for air-breathing. *Zoomorphology* 112:39-49.

Fiala JC. 2005. Reconstruct: a free editor for serial section microscopy. *Journal of microscopy* 218:52-61.

Fischer FP, Alger M, Cieslar D, and Krafczyk HU. 1990. The chiton gill: Ultrastructure in *Chiton olivaceus* (Mollusca, Polyplacophora). *Journal of Morphology* 204:75-87.

Flik G, and Verbost P. 1993. Calcium transport in fish gills and intestine. *Journal of Experimental Biology* 184:17-29.

Foley DA, and Cheng TC. 1977. Degranulation and other changes of molluscan granulocytes associated with phagocytosis. *Journal of Invertebrate Pathology* 29:321-325.

638 Giraud-Billoud M, Abud M, Cueto J, Vega I, and Castro-Vazquez A. 2011. Uric acid deposits
639 and estivation in the invasive apple-snail, *Pomacea canaliculata*. *Comparative &*
640 *Biochemical Physiology Part A* 158:506-512.
641 Giraud-Billoud M, Vega IA, Rinaldi Tosi ME, Abud MA, Calderón ML, and Castro-Vazquez A.
642 2013. Antioxidant and molecular chaperone defenses during estivation and arousal in the
643 South American apple-snail *Pomacea canaliculata*. *Journal of Experimental Biology*
644 216:614-622.
645 Graham J, Lee H, and Wegner N. 2007. Transition from water to land in an extant group of
646 fishes: Air breathing and the acquisition sequence of adaptations for amphibious life in
647 Oxudercine gobies. In: Fernandes MN, Rantin FT, Mogens LG, and Kapoor B, eds. *Fish*
648 *Respiration and Environment*: Science Publishers, 255-288.
649 Gregory M, George R, and McClurg T. 1996. The architecture and fine structure of gill filaments
650 in the brown mussel, *Perna perna*. *African Zoology* 31:193-207.
651 Haszprunar G. 1988. On the origin and evolution of major gastropod groups, with special
652 reference to the Streptoneura. *Journal of Molluscan Studies* 54:367-441.
653 Haszprunar G. 1992. The first molluscs - small animals. *Bolletino di Zoologia (Italian Journal of*
654 *Zoology)* 59:1-16.
655 Hayes KA, Burks R, Castro-Vazquez A, Darby PC, Heras H, Martín PR, Qiu J-W, Thiengo SC,
656 Vega IA, Yusa Y, Wada T, Burela S, Cadierno MP, Cueto JA, Dellagnola FA, Dreon
657 MS, Frassa VM, Giraud-Billoud M, Godoy MS, Ituarte S, Koch E, Matsukura K,
658 Pasquevich Y, Rodriguez C, Saveanu L, Seuffert ME, Strong EE, Sun J, Tamburi NE,
659 Tiecher MJ, Turner RL, Valentine-Darby P, and Cowie RH. 2015. Insights from an
660 integrated view of the biology of apple snails (Caenogastropoda: Ampullariidae).
661 *Malacologia* 58:245-302.
662 Hayes KA, Cowie RH, Jørgensen A, Schultheiß R, Albrecht C, and Thiengo SC. 2009a.
663 Molluscan models in evolutionary biology: Apple snails (Gastropoda: Ampullariidae) as
664 a system for addressing fundamental questions. *American Malacological Bulletin* 27:47-
665 58.
666 Hayes KA, Cowie RH, and Thiengo SC. 2009b. A global phylogeny of apple snails: Gondwanan
667 origin, generic relationships, and the influence of outgroup choice (Caenogastropoda:
668 Ampullariidae). *Biological Journal of the Linnean Society* 98:61-76.
669 Housset C, Chrétien Y, Debray D, and Chignard N. 2016. Functions of the gallbladder.
670 *Comprehensive Physiology* 6:1549-1577.
671 Hughes G, and Morgan M. 1973. The structure of fish gills in relation to their respiratory
672 function. *Biological Reviews* 48:419-475.
673 Hylton Scott MI. 1957. Estudio morfológico y taxonómico de los ampulláridos de la República
674 Argentina. *Revista del Museo Argentino de Ciencias Naturales "Bernardino Rivadavia"*
675 3:233-333.
676 Hyman LH. 1967. *The Invertebrates*. New York: McGraw-Hill.
677 Innes A, and Taylor E. 1986. The evolution of air-breathing in crustaceans: A functional analysis
678 of branchial, cutaneous and pulmonary gas exchange. *Comparative Biochemistry and*
679 *Physiology Part A: Physiology* 85:621-637.
680 Ip JC, Mu H, Zhang Y, Sun J, Heras H, Chu KH, and Qiu J-W. 2019. Understanding the
681 transition from water to land: Insights from multi-omic analyses of the perivitelline fluid
682 of apple snail eggs. *Journal of Proteomics* 194:79-88.

683 Jonas M. 1986. Ultrastructural of the gill epithelia of the dorid nudibranchs *Archidoris*
684 *pseudoargus* (von Rapp, 1827) and *Peltodoris atromaculata* Bergh, 1880 (Gastropoda:
685 Opisthobranchia). *The Veliger* 29:207-216.
686 Jonz MG, and Nurse CA. 2003. Neuroepithelial cells and associated innervation of the zebrafish
687 gill: a confocal immunofluorescence study. *Journal of Comparative Neurology* 461:1-17.
688 Jonz MG, and Nurse CA. 2006. Epithelial mitochondria-rich cells and associated innervation in
689 adult and developing zebrafish. *Journal of Comparative Neurology* 497:817-832.
690 Jonz MG, and Zaccone G. 2009. Nervous control of the gills. *Acta Histochemica* 111:207-216.
691 Knight J, and Knight R. 1986. The blood vascular system of the gills of *Pholas dactylus* L.
692 (Mollusca, Bivalvia, Eulamellibranchia). *Philosophical Transactions of the Royal Society*
693 *of London B* 313:509-523.
694 Koch E, Winik BC, and Castro-Vazquez A. 2009. Development beyond the gastrula stage and
695 digestive organogenesis in the apple-snail *Pomacea canaliculata* (Architaenioglossa,
696 Ampullariidae). *Biocell* 33:49-65.
697 Laurent P, and Dunel S. 1980. Morphology of gill epithelia in fish. *American Journal of*
698 *Physiology-Regulatory, Integrative and Comparative Physiology* 238:R147-R159.
699 Le Pennec M, Beninger P, and Herry A. 1988. New observations of the gills of *Placopecten*
700 *magellanicus* (Mollusca: Bivalvia), and implications for nutrition. *Marine Biology*
701 98:229-237.
702 Lewinson D, Rosenberg M, and Warburg M. 1987. Ultrastructural and ultracytochemical studies
703 of the gill epithelium in the larvae of *Salamandra salamandra* (Amphibia, Urodela).
704 *Zoomorphology* 107:17-25.
705 Lindberg DR, and Ponder WF. 2001. The influence of classification on the evolutionary
706 interpretation of structure a re-evaluation of the evolution of the pallial cavity of
707 gastropod molluscs. *Organisms Diversity & Evolution* 1:273-299.
708 Lindberg DR, and Sigwart JD. 2015. What is the molluscan osphradium? A reconsideration of
709 homology. *Zoologischer Anzeiger-A Journal of Comparative Zoology* 256:14-21.
710 Low W, Lane D, and Ip Y. 1988. A comparative study of terrestrial adaptations of the gills in
711 three mudskippers: *Periophthalmus chrysospilos*, *Boleophthalmus boddaerti*, and
712 *Periophthalmodon schlosseri*. *Biological Bulletin*:434-438.
713 Luquet C, Genovese G, Rosa G, and Pellerano G. 2002. Ultrastructural changes in the gill
714 epithelium of the crab *Chasmagnathus granulatus* (Decapoda: Grapsidae) in diluted and
715 concentrated seawater. *Marine Biology* 141:753-760.
716 Lutfy RG, and Demian ES. 1965. The histology of the respiratory organs of *Marisa cornuarietis*
717 (L.). *Arkiv för Zoologi* 18:51-71.
718 Maina JN. 1990. The morphology of the gills of the freshwater African crab *Potamon niloticus*
719 (Crustacea: Brachyura: Potamonidae): A scanning and transmission electron microscopic
720 study. *Journal of Zoology* 221:499-515.
721 Maina JN. 2000a. Comparative respiratory morphology: themes and principles in the design and
722 construction of the gas exchangers. *Anatomical Record (New Anatomist)* 261:25-44.
723 Maina JN. 2000b. Is the sheet-flow design a 'frozen core'(a Bauplan) of the gas exchangers?:
724 Comparative functional morphology of the respiratory microvascular systems: illustration
725 of the geometry and rationalization of the fractal properties. *Comparative Biochemistry*
726 *and Physiology-Part A: Molecular & Integrative Physiology* 126:491-515.
727 Maina JN. 2002a. Sheet flow design in the vasculature of gas exchangers. In: Maina JN, ed.
728 *Fundamental Structural Aspects and Features in the Bioengineering of the Gas*

729 *Exchangers: Comparative Perspectives*. Berlin; Heidelberg; New York; Barcelona; Hong
730 Kong; London; Milan; Paris; Tokyo: Springer, 47-49.
731 Maina JN. 2002b. Structure, function and evolution of the gas exchangers: comparative
732 perspectives. *Journal of Anatomy* 201:281-304.
733 Maina JN, and West JB. 2005. Thin and strong! The bioengineering dilemma in the structural
734 and functional design of the blood-gas barrier. *Physiological Reviews* 85:811-844.
735 Manganaro M, Laurà R, Guerrera MC, Lanteri G, Zaccone D, and Marino F. 2012. The
736 morphology of gills of *Haliotis tuberculata* (Linnaeus, 1758). *Acta Zoologica* 93:436-
737 443.
738 McDonald DG, Cavdek V, and Ellis R. 1991. Gill design in freshwater fishes: interrelationships
739 among gas exchange, ion regulation, and acid-base regulation. *Physiological Zoology*
740 64:103-123.
741 McNamara JC, and Faria SC. 2012. Evolution of osmoregulatory patterns and gill ion transport
742 mechanisms in the decapod Crustacea: A review. *Journal of Comparative Physiology B*
743 182:997-1014.
744 Mohandas A, Cheng TC, and Cheng JB. 1985. Mechanism of lysosomal enzyme release from
745 *Mercenaria mercenaria* granulocytes: A scanning electron microscope study. *Journal of*
746 *Invertebrate Pathology* 46:189-197.
747 Mu H, Sun J, Heras H, Chu KH, and Qiu J-W. 2017. An integrated proteomic and transcriptomic
748 analysis of perivitelline fluid proteins in a freshwater gastropod laying aerial eggs.
749 *Journal of Proteomics* 155:22-30.
750 Nakao T. 1975. The fine structure and innervation of gill lamellae in *Anodonta*. *Cell and Tissue*
751 *Research* 157:239-254.
752 Nicaise G. 1973. The gliointerstitial system of molluscs. *International Review of Cytology*.
753 Academic Press: Elsevier, 251-332.
754 Nuwayhid M, Davies PS, and Elder H. 1978. Gill structure in the common limpet *Patella*
755 *vulgata*. *Journal of the Marine Biological Association of the United Kingdom* 58:817-
756 823.
757 Ottaviani E. 1991. Tissue distribution and levels of natural and induced serum lysozyme
758 immunoreactive molecules in a freshwater snail. *Tissue and Cell* 23:317-324.
759 Pickett JA, and Edwardson JM. 2006. Compound exocytosis: mechanisms and functional
760 significance. *Traffic* 7:109-116.
761 Ponder WF, and Lindberg DR. 1997. Towards a phylogeny of gastropod molluscs: an analysis
762 using morphological characters. *Zoological Journal of the Linnean Society* 119:83-265.
763 Prashad B. 1925. Anatomy of the common Indian apple-snail, *Pila globosa*. *Memoirs of the*
764 *Indian Museum* 8:91-154.
765 Ranjah A. 1942. The embryology of the Indian apple-snail, *Pila globosa* (Swainson) (Mollusca,
766 Gastropoda). *Records of the Indian Museum* 44:217-322.
767 Rebelo MdF, Figueiredo EdS, Mariante RM, Nóbrega A, de Barros CM, and Allodi S. 2013.
768 New insights from the oyster *Crassostrea rhizophorae* on bivalve circulating hemocytes.
769 *PLoS ONE* 8:e57384.
770 Ridewood WG. 1903. On the structure of the gills of the Lamellibranchia. *Philosophical*
771 *Transactions of the Royal Society of London* 195:147-284.
772 Rodriguez C, Prieto GI, Vega IA, and Castro-Vazquez A. 2018. Assessment of the kidney and
773 lung as immune barriers and hematopoietic sites in the invasive apple snail *Pomacea*
774 *canaliculata*. *PeerJ* 6:e5789. 10.7717/peerj.5789

775 Ruthensteiner B. 1997. Homology of the pallial and pulmonary cavity of gastropods. *Journal of*
776 *Molluscan Studies* 63:353-367.
777 Ruthensteiner B, and HEß M. 2008. Embedding 3D models of biological specimens in PDF
778 publications. *Microscopy Research and Technique* 71:778-786.
779 Salvini-Plawen L, and Haszprunar G. 1987. The Vetigastropoda and the systematics of
780 streptoneurous Gastropoda (Mollusca). *Journal of Zoology* 211:747-770.
781 Semper K. 1881. *Animal life as affected by the natural conditions of existence*. New York: D.
782 Appleton and Co.
783 Seuffert ME, and Martín PR. 2010. Dependence on aerial respiration and its influence on
784 microdistribution in the invasive freshwater snail *Pomacea canaliculata*
785 (Caenogastropoda, Ampullariidae). *Biological Invasions* 12:1695-1708. 10.1007/s10530-
786 009-9582-5
787 Stein JL, Cary SC, Hessler RR, Vetter RD, Felbeck H, Ohta S, and Childress JJ. 1988.
788 Chemoautotrophic symbiosis in a hydrothermal vent gastropod. *The Biological Bulletin*
789 174:373-378.
790 Stern DL. 2013. The genetic causes of convergent evolution. *Nature Reviews Genetics* 14:751-
791 764.
792 Sun J, Mu H, Ip JCH, Li R, Xu T, Accorsi A, Sánchez Alvarado A, Ross E, Lan Y, Castro-
793 Vazquez A, Vega IA, Heras H, Ituarte S, Bocxclaer Bv, Hayes KA, Cowie RH, Zhao Z,
794 Zhang Y, Qian P-Y, and Qiu J-W. 2019. Signatures of divergence, invasiveness, and
795 terrestrialization revealed by four apple snail genomes. *Molecular Biology and Evolution*
796 msz084, https://doi.org/10.1093/molbev/msz084.
797 Taylor P, and Andrews EB. 1987. Tissue adenosine-triphosphatase activities of the gill and
798 excretory system in mesogastropod molluscs in relation to osmoregulatory capacity.
799 *Comparative Biochemistry and Physiology Part A: Physiology* 86:693-696.
800 Ueshima E, and Yusa Y. 2015. Antipredator behaviour in response to single or combined
801 predator cues in the apple snail *Pomacea canaliculata*. *Journal of Molluscan Studies*
802 81:51-57.
803 Vega IA, Damborenea M, Gamarra-Luques C, Koch E, Cueto J, and Castro-Vazquez A. 2006.
804 Facultative and obligate symbiotic associations of *Pomacea canaliculata*
805 (Caenogastropoda, Ampullariidae). *Biocell* 30:367-375.
806 Wanichanon C, Laimek P, Linthong V, Sretarugsa P, Kruatrachue M, Upatham ES, Poomtong T,
807 and Sobhon P. 2004. Histology of hypobranchial gland and gill of *Haliotis asinina*
808 Linnaeus. *Journal of Shellfish Research* 23:1107-1113.
809 Wilson JM, and Laurent P. 2002. Fish gill morphology: inside out. *Journal of Experimental*
810 *Zoology* 293:192-213.
811 Windoffer R, and Giere O. 1997. Symbiosis of the hydrothermal vent gastropod *Ifremeria*
812 *nautilei* (Provannidae) with endobacteria-structural analyses and ecological
813 considerations. *The Biological Bulletin* 193:381-392.
814 Yonge CM. 1947. The pallial organs in the aspidobranch Gastropoda and their evolution
815 throughout the Mollusca. *Philosophical Transactions of the Royal Society of London*
816 *Series B, Biological Sciences* 232:443-518.
817 Yu AS. 2017. Paracellular transport as a strategy for energy conservation by multicellular
818 organisms? *Tissue Barriers* 5:2509-2518.

819

820

Figure 1

The gill and the pallial complex.

(A) Diagram of the pallial cavity of a male animal, opened as indicated in the thumbnail sketch at the right lower corner. (B) Panoramic section of the single row of rather parallel leaflets of the monopectinate gill that hang from the gill's base, below the outer mantle; the approximate position of this section is indicated in the thumbnail sketch at the right lower corner. (C) (D) (E). Haematoxylin–eosin. Scale bar represents 1 mm. Abbreviations: abv, afferent branchial vessel; anu, anus; gil, gill; dig, digestive gland; epb, efferent pulmobranchial vessel; ime, inner mantle epithelium; kid, kidney; lft, gill leaflets; lng, lung; med, mantle edge; mth, mouth; npo, nephropore; ome, outer mantle epithelium; osp, osphradium; pec, penial complex; pes, penial sheath; pfo, pallial fold; pne, pneumostome; pod, foot; rnl, right nuchal lobe; prc, pericardium; pro, prostate; sip, siphon; ten, tentacle; tes, testis; urt, ureter; vap, ventral afferent pulmonary vessel.

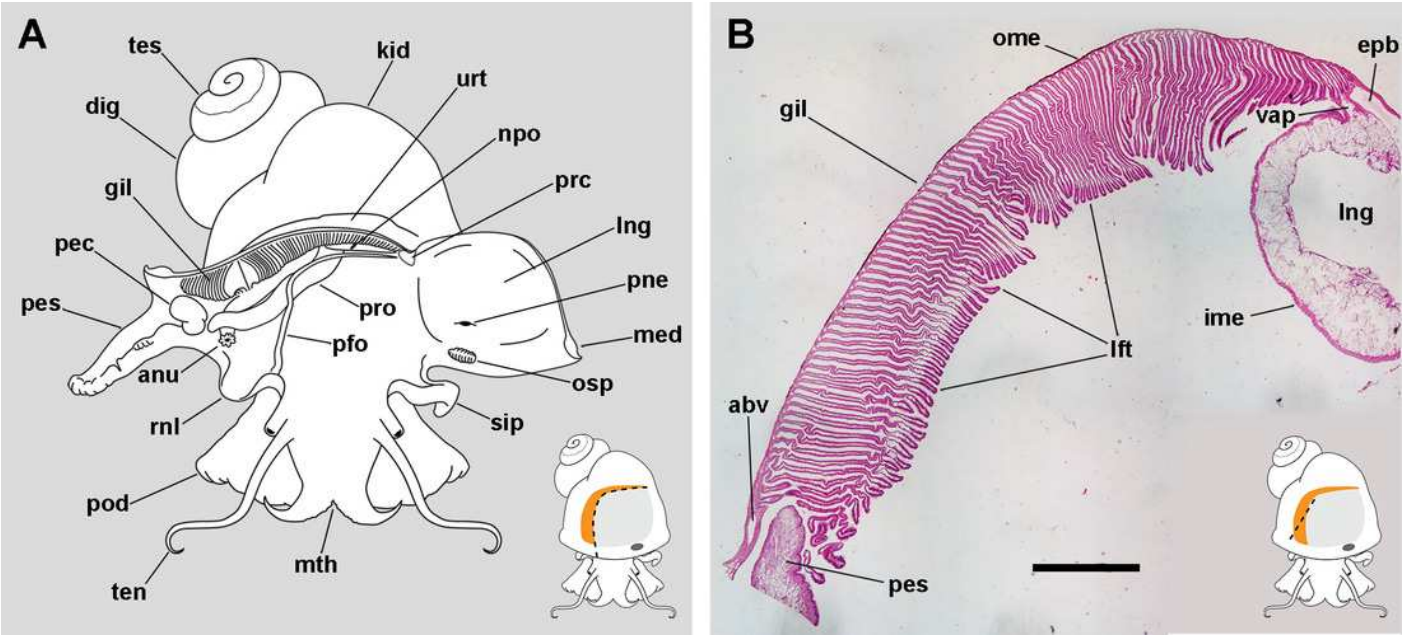

Figure 2

Computerised 3D rendering of the blood system of the gill.

(A) Dorsal view of the pallial complex. The gill (orange) occupies the right and posterior portion of the roof of the pallial cavity, bordering the lung (which is collapsed, see Methods) and the ureter. (B) Lateral view of a single gill leaflet. (C) The gill's blood supply; three gill leaflets are indicated by asterisks. (D) Blood sinuses in a single gill leaflet. (E) Diagram of the proposed blood flow to and from the gill. (F) Diagram of proposed blood flow within a gill leaflet. Scale bars represent: (A and C) 1 mm; (B and D) 500 µm. Abbreviations: abv, afferent branchial vessel; apv, afferent pulmonary vessel; aur, auricle; bls, basal leaflet sinus; gil, gill; epb, efferent pulmobranchial vessel; euv, efferent ureteral vessel (=efferent renal vein); lfs, laminar leaflet sinus; lft, gill leaflet; lng, lung; med, mantle edge; mls, marginal leaflet sinus; npo, nephropore; osp, osphradium; pne, pneumostome; rct, rectum; rps, right pallial sinus; rsi, rectal sinus; urt, ureter; vap, ventral afferent pulmonary vessel.

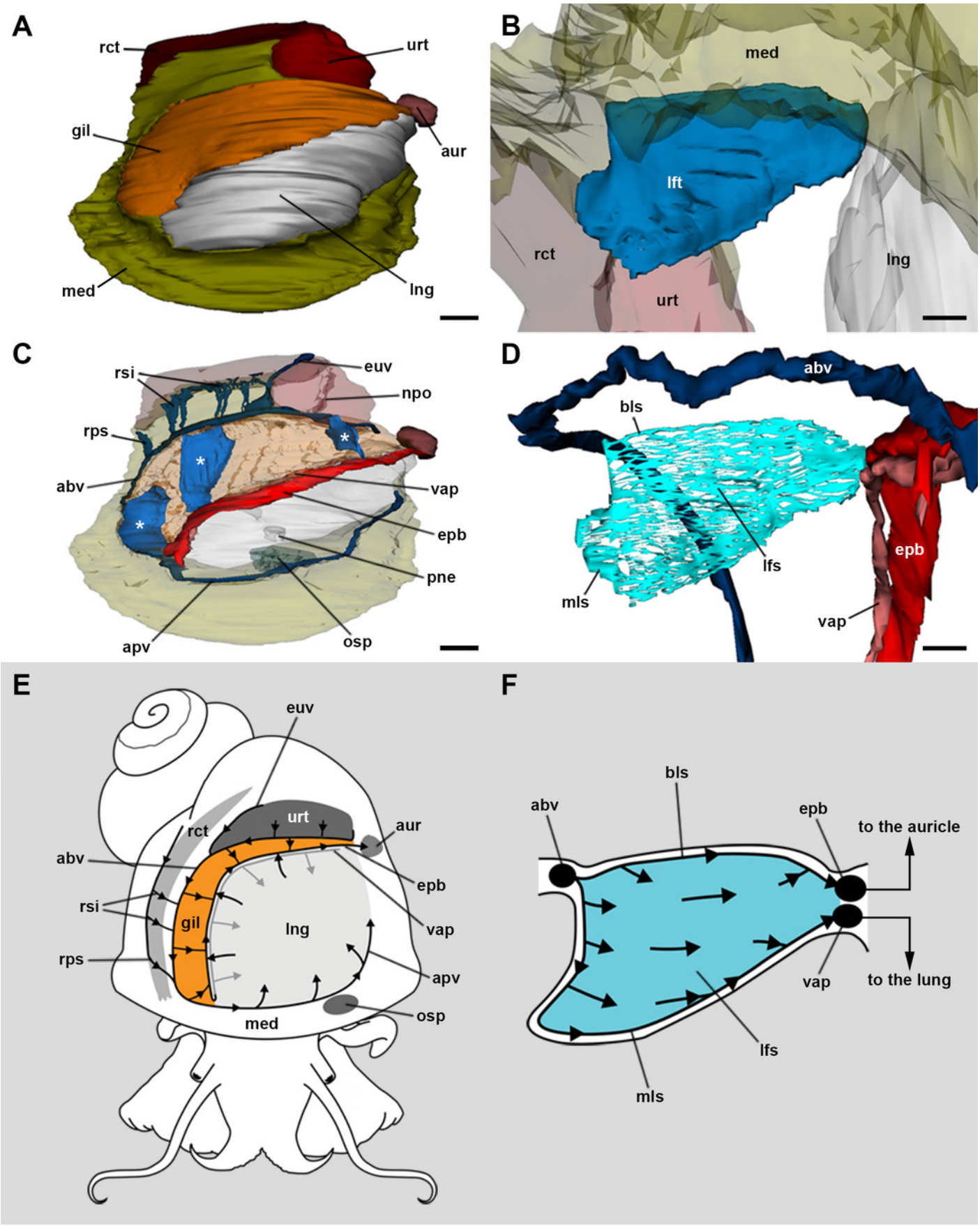
A
rct
urt
gil
aur
med
lng
B
med
lft
rct
lng
urt
C
rsi
euv
npo
rps
*
*
*
abv
vap
epb
pne
apv
osp
D
abv
bls
lfs
epb
mls
vap
E
euv
urt
rct
aur
abv
epb
rsi
gil
lng
vap
rps
apv
osp
med
F
bls
abv
epb
to the auricle
vap
to the lung
lfs
mls

Figure 3

Gill innervation.

(A) Diagram showing the major ganglia (grey), the nerves, and the accessory ganglia supplying branchial innervation. The gill is innervated from the supraoesophageal ganglion by branches of the branchial nerve (pink). The branchial base nerve originates in the accessory visceral ganglion (violet). The copulatory ganglion may also contribute to branchial innervation (green). (B) Diagram of nerves within each gill leaflet and presumptive origin of the fine innervation (dashed lines). (C) Panoramic section of the gill, showing the branchial base nerve lying alongside the afferent branchial vessel. (D) Detail of the penial complex, showing the copulatory ganglion in the proximity of the branchial base nerve. (E) Detail of the gill base showing the branchial base nerve and the afferent branchial vessel. (F) Detail showing the branchial base nerve in the proximity of the efferent ureteral vessel. Haematoxylin–eosin; panels D–F correspond to sections adjacent to that in panel C. Scale bars represent: (C) 1 cm; (D) 1 mm; (E–F) 500 µm. Abbreviations: abv, afferent branchial vessel; avg, accessory visceral ganglion; bbn, branchial base nerve; brn, branchial nerve; cog, copulatory ganglion; euv, efferent ureteral vessel (=efferent renal vein); lfn, leaflet nerve; lft, gill leaflet; ome, outer mantle epithelium; osg, osphradial ganglion; pec, penial complex; pes, penial sheath; rpg, right pleural ganglion; rps, right pallial sinus; spg, supraoesophageal ganglion; svl, supraoesophageal portion of the visceral loop; urt, ureter; vig, visceral ganglion.

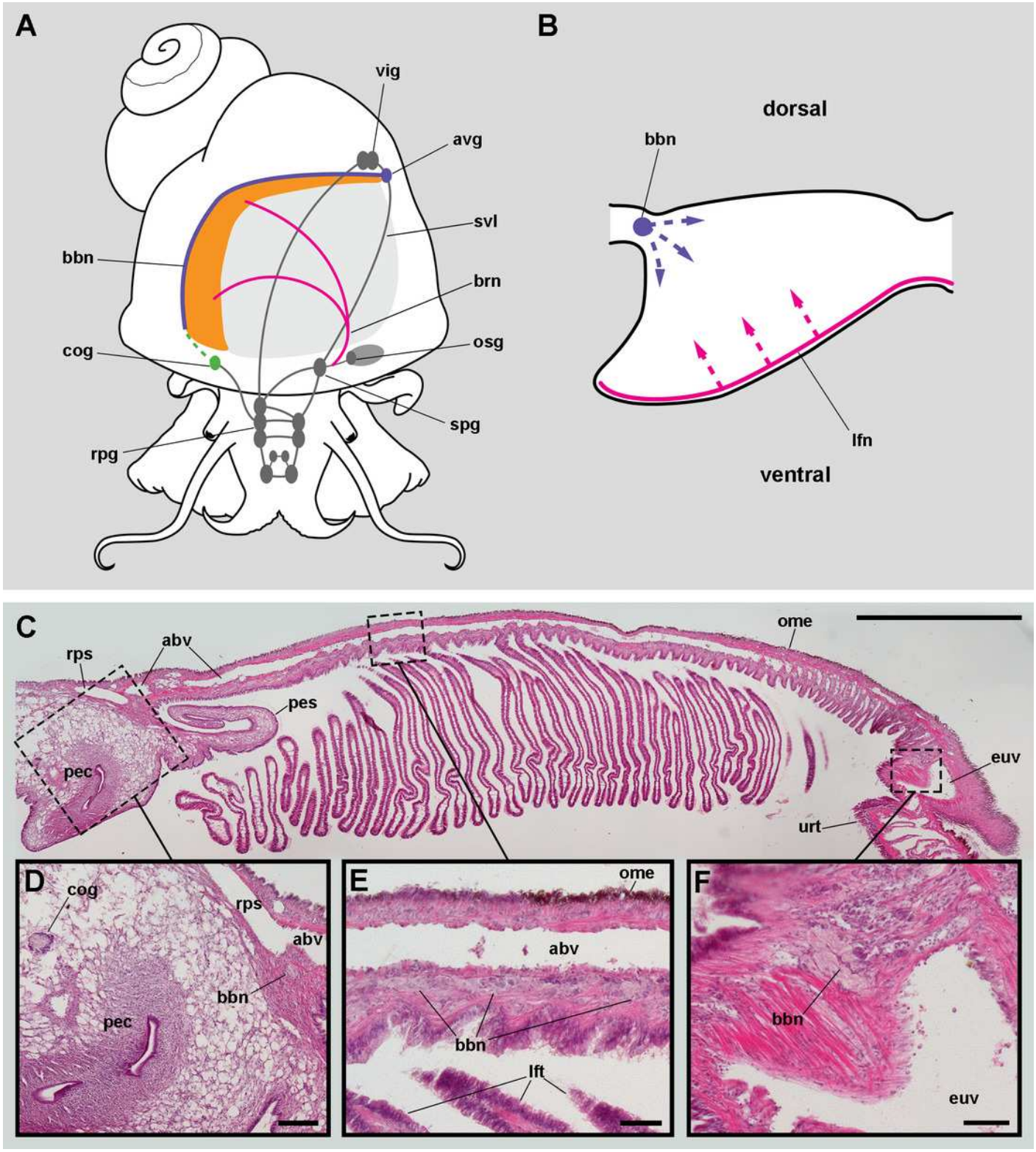
A
vig
avg
svl
bbn
brn
cog
osg
spg
rpg
B
dorsal
bbn
lfn
ventral
C
rps
abv
ome
pes
pec
euv
urt
D
cog
rps
abv
bbn
pec
E
ome
abv
bbn
lft
F
bbn
euv

Figure 4

The gill leaflets and their regions (light microscopy).

(A) Diagram of the four regions of the gill leaflets, which differ in the cell types of its covering epithelium and underlying structures. (B–C) Region I occupies the largest part of the leaflet, while regions II–IV. (D–E) constitute its thickened margin. Scale bars represent 20 µm. Haematoxylin-eosin or toluidine blue. Abbreviations: bls, basal leaflet sinus; cil, cilia; fml, fibromuscular layer; gra, granulocytes; ics, intercellular spaces; lfn, leaflet nerve; lfs, laminar leaflet sinus; mls, marginal leaflet sinus; nuc, epithelial cell nuclei; ome, outer mantle epithelium; rod, supporting rod; sec, secretory cells; tra, trabeculae.

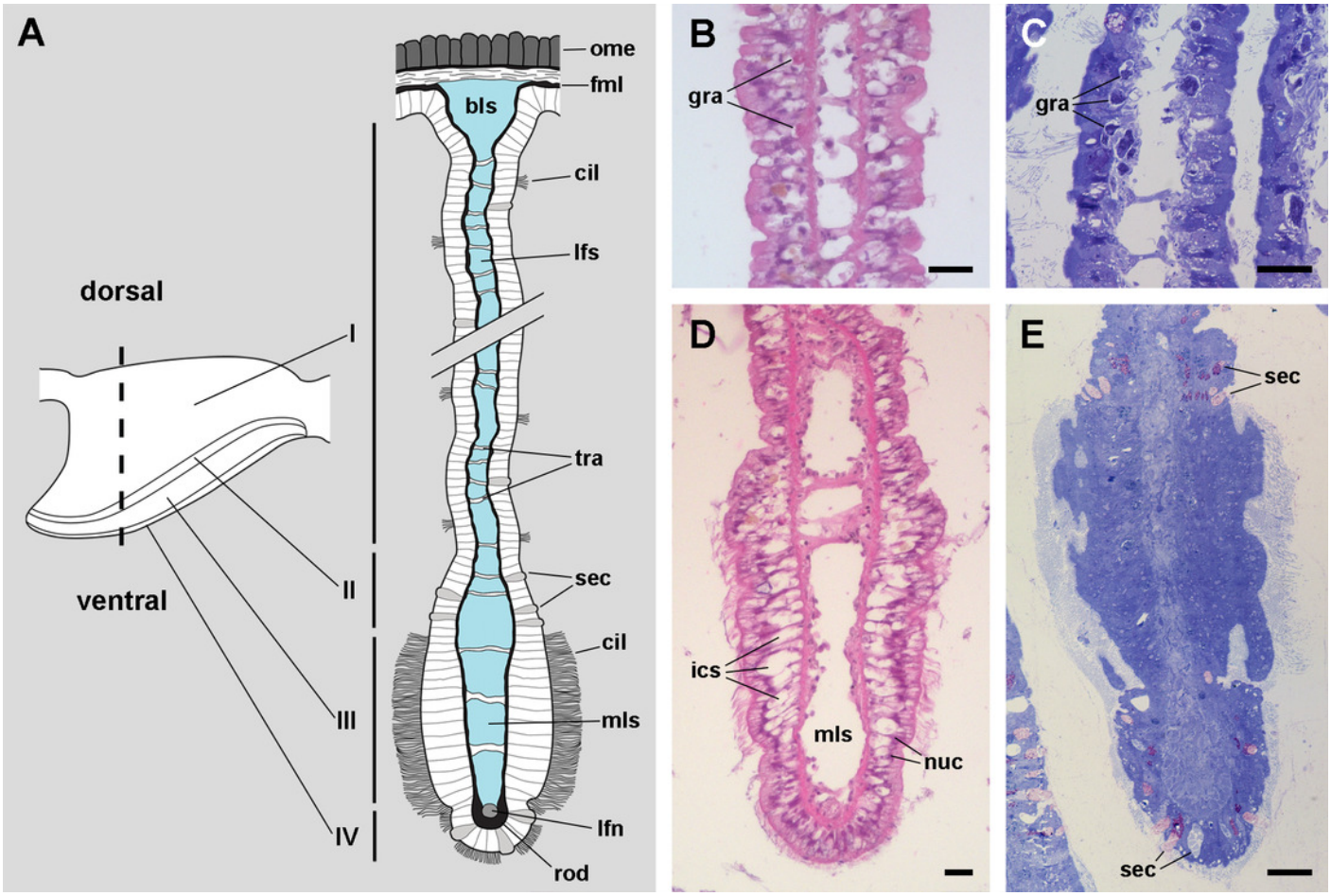

Figure 5

Apical specialisations on the gill surface (scanning electron microscopy).

(A) Three adjacent gill leaflets, two of them sectioned to show the laminar leaflet sinus. Regions described in Figure 4A are indicated in the thumbnail sketch. (B) Region I exhibiting the cilia of α-cells and the ramified microvilli of β-cells. (C) Region III exhibiting the long cilia of C2 cells with the characteristic membrane blebs. (D) Region IV exhibiting bundles of the short cilia of C1 cells, and interspersed spaces showing the microvilli of α-cells. (E) A cut through region I of a gill leaflet, showing the laminar leaflet sinus, the trabeculae traversing it, and the covering leaflet epithelia showing α-cells, β-cells and C1 cells. Scale bars represent: (A) 200 µm; (B) 10 µm; (C–E) 2 µm. Abbreviations: α-c, α-cells; β-c, β-cells; C1, short cilia cells; lfs, laminar leaflet sinus; mbl, membrane blebs on the long cilia; tra, trabeculae.

**Note: Auto Gamma Correction was used for the image. This only affects the reviewing manuscript. See original source image if needed for review.*

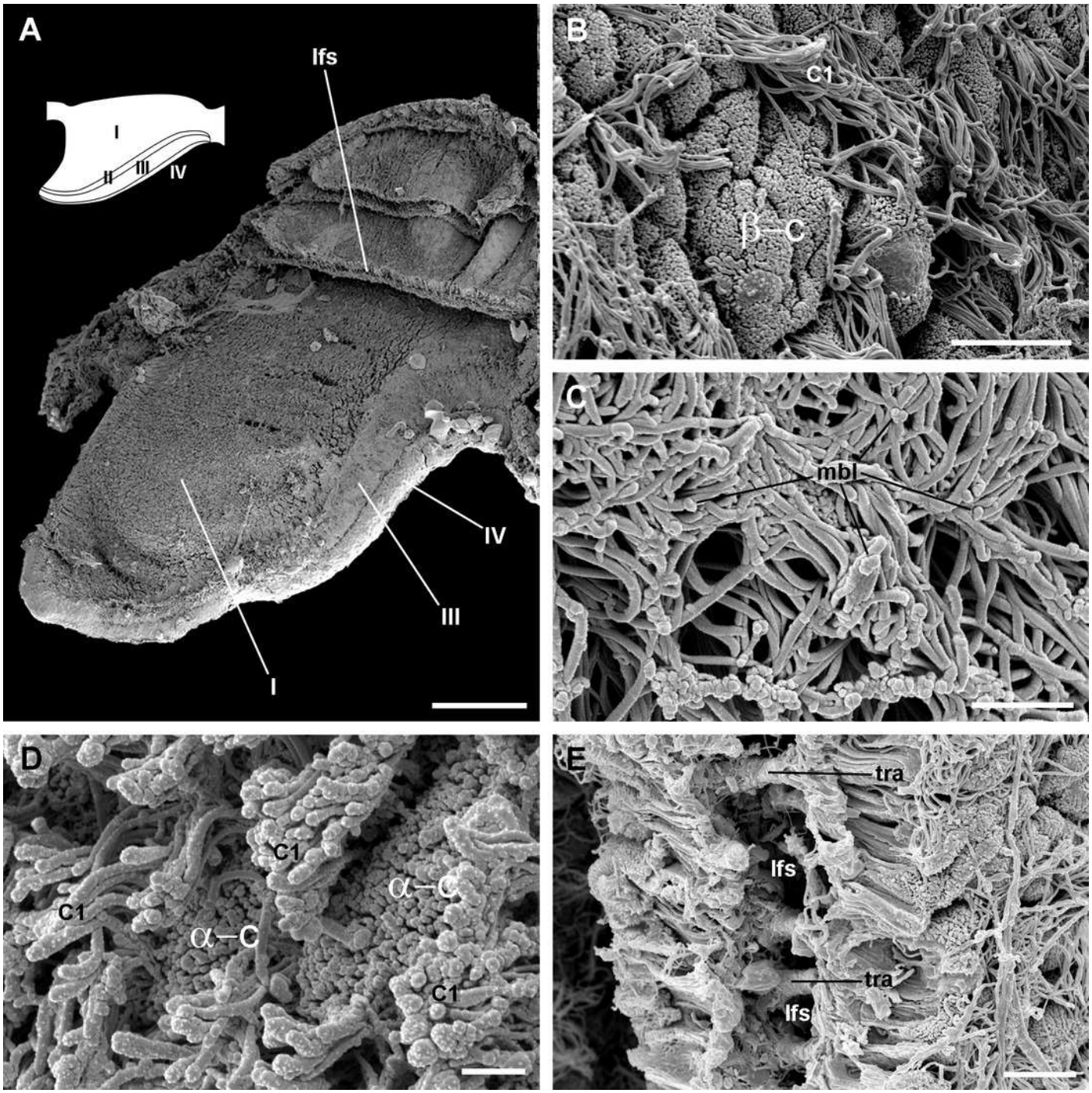
A
lfs
I
II
III
IV
IV
III
I
B
C1
β–C
C
mbl
D
C1
C1
α–C
α–C
C1
E
tra
lfs
tra
lfs

Figure 6

The supporting rod and the leaflet nerve (light and electron microscopy).

(A) Margin of a gill leaflet showing the covering epithelium, the supporting rod and the leaflet nerve. Toluidine blue. (B) Razor blade cuts of three gill leaflets showing the supporting rods as well-defined units beneath the covering epithelium. Scanning electron microscopy. (C) Tangential section of the leaflet border showing two muscular cells pertaining to the supporting rod and a fairly longitudinal section of the leaflet nerve. Transmission electron microscopy. (D) A high magnification of the leaflet nerve showing tightly packed neurites containing neurotubules, clear vesicles or electron-dense granules of different sizes. (E) A section through the supporting rod showing large muscle fibres containing myofibrils, and that are embedded in a collagen matrix where glial processes are found. Arrowheads indicate the basal lamina of the covering epithelium. Scale bars represent: (A) 10 µm; (B) 25 µm; (C–D) 1 µm; (E) 250 nm. Abbreviations: C1, short cilia cells; col, collagen matrix; gcp, glial cell process; gra, granulocyte; msc, muscle cell; mye, myeloid body; lfn, leaflet nerve; rod, supporting rod; S1, metachromatic secretory cells; S2, orthochromatic secretory cells.

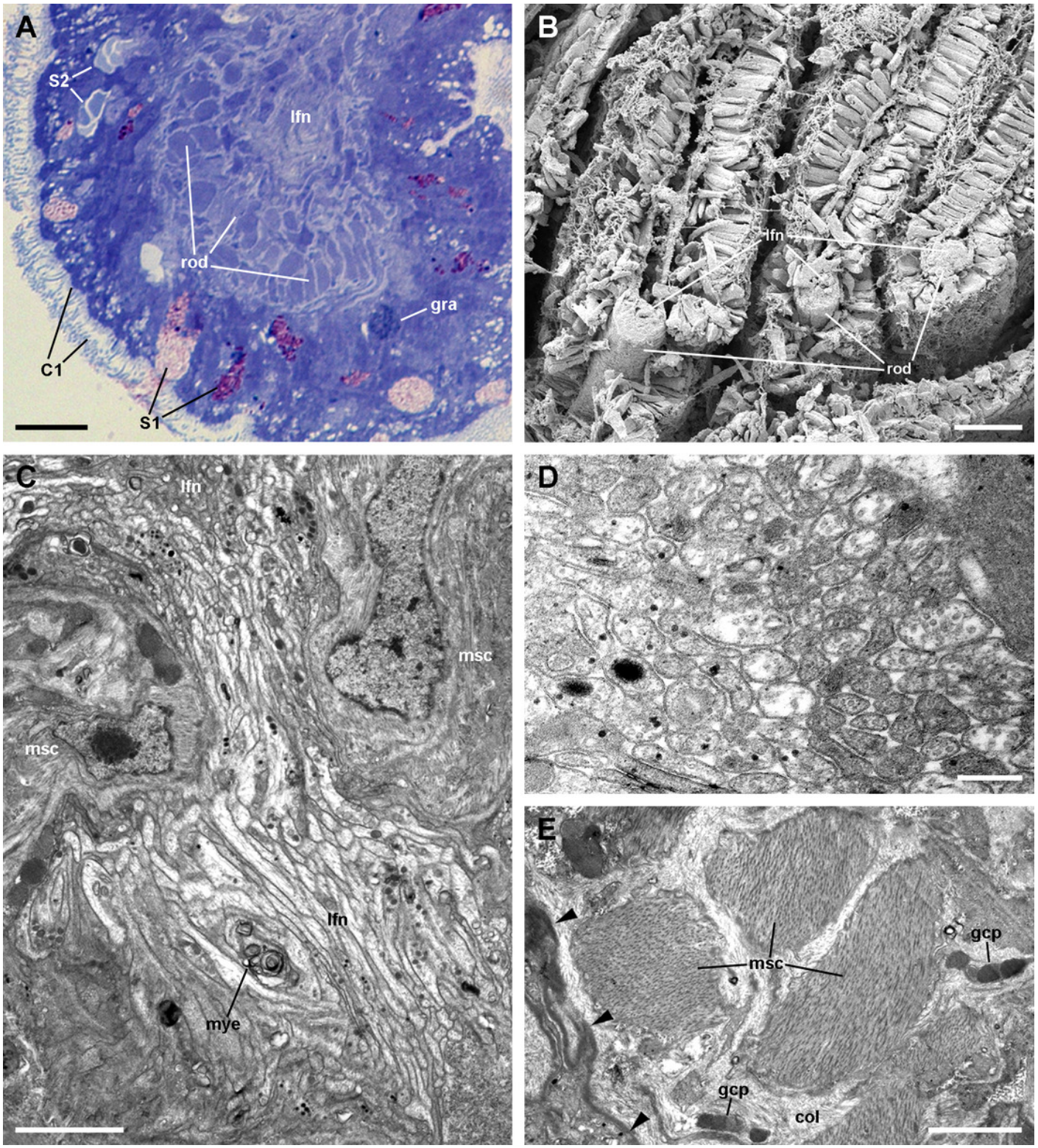
A
S2
lfn
rod
gra
C1
S1
B
lfn
rod
C
lfn
msc
msc
lfn
mye
D
E
gcp
msc
gcp
col

Figure 7

Mitochondria-rich cells in region I of the gill leaflets (diagram).

The two main cell types found in region I are α- and β-cells. In addition, granulocytes occur within epithelial intercellular spaces. Abbreviations: adh, adherent junction; α-c, alpha-cell; β-c, beta-cell; bla, basal lamina; dtu, bundles of electron-dense tubules; gra, granulocyte; grn, R granules; fgr, fibrogranular material; gly, glycogen deposit; icc, intercellular canaliculi; ics, intercellular space; mlb, multilamellar bodies; mvb, multivesicular bodies; mvi, microvilli; mye, myeloid bodies; neu, neurite bundle; sep, septate junction; tep, thin epithelial projections; tub, tubular system.

**Note: Auto Gamma Correction was used for the image. This only affects the reviewing manuscript. See original source image if needed for review.*

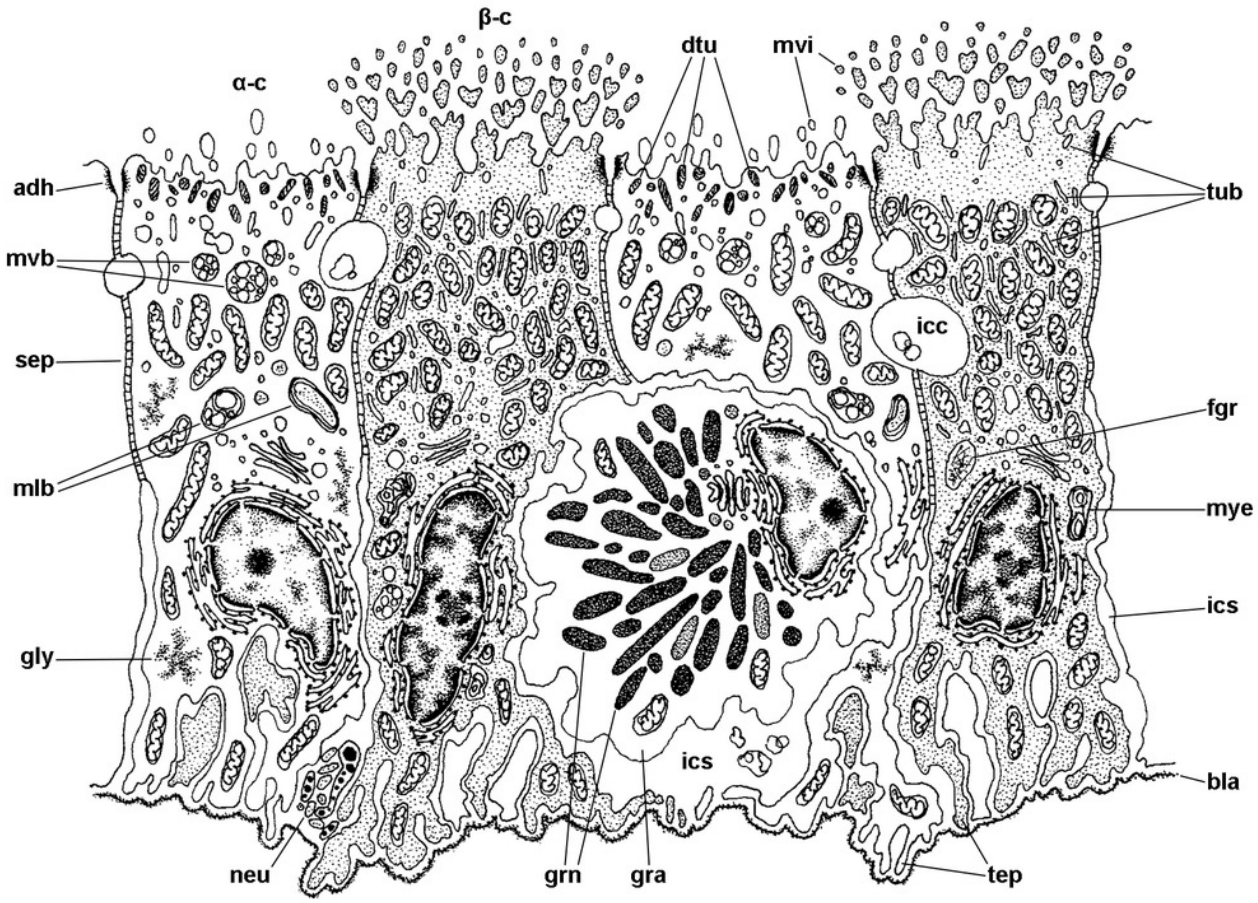

Figure 8

Mitochondria-rich cells in region I of the gill leaflets (transmission electron microscopy).

(A) Alpha-cells exhibit few and short microvilli, numerous and long mitochondria with well-defined cristae, and glycogen deposits. Their nuclei are euchromatic with conspicuous nucleoli. (B) Apically, α-cells show numerous membrane-bound bundles of electron-dense tubules/filaments, and a well-developed vesicular system, including multivesicular bodies. (C) Multilamellar bodies and Golgi bodies are found close to the nucleus. (D) Contrasting with α-cells, β-cells have numerous and ramified microvilli. These cells also have numerous tightly-packed mitochondria that fill almost all the cytoplasm. The nuclei are heterochromatic. (E) Beta-cells show an extensive tubular system between the mitochondria. (F) A β-cell showing multivesicular bodies and presumptively degenerative bodies, such as myeloid bodies and fibrogranular material. Scale bars represent: (A) 1 µm; (B) 200 nm; (C) 250 nm; (D) 1 µm; (E) 500 nm; (F) 250 nm. Abbreviations: α-c, alpha-cell; β-c, beta-cell; dtu, bundles of electron-dense tubules; fgr, fibrogranular material; gly, glycogen deposit; gol, Golgi body; gra, granulocyte; icc, intercellular canaliculi; mit, mitochondria; mlb, multilamellar body; mvb, multivesicular body; mvi, microvilli; mye, myeloid body; nuc, cell nucleus; rer, rough endoplasmic reticulum; tep, thin epithelial projections; tub, tubular-vesicular system.

**Note: Auto Gamma Correction was used for the image. This only affects the reviewing manuscript. See original source image if needed for review.*

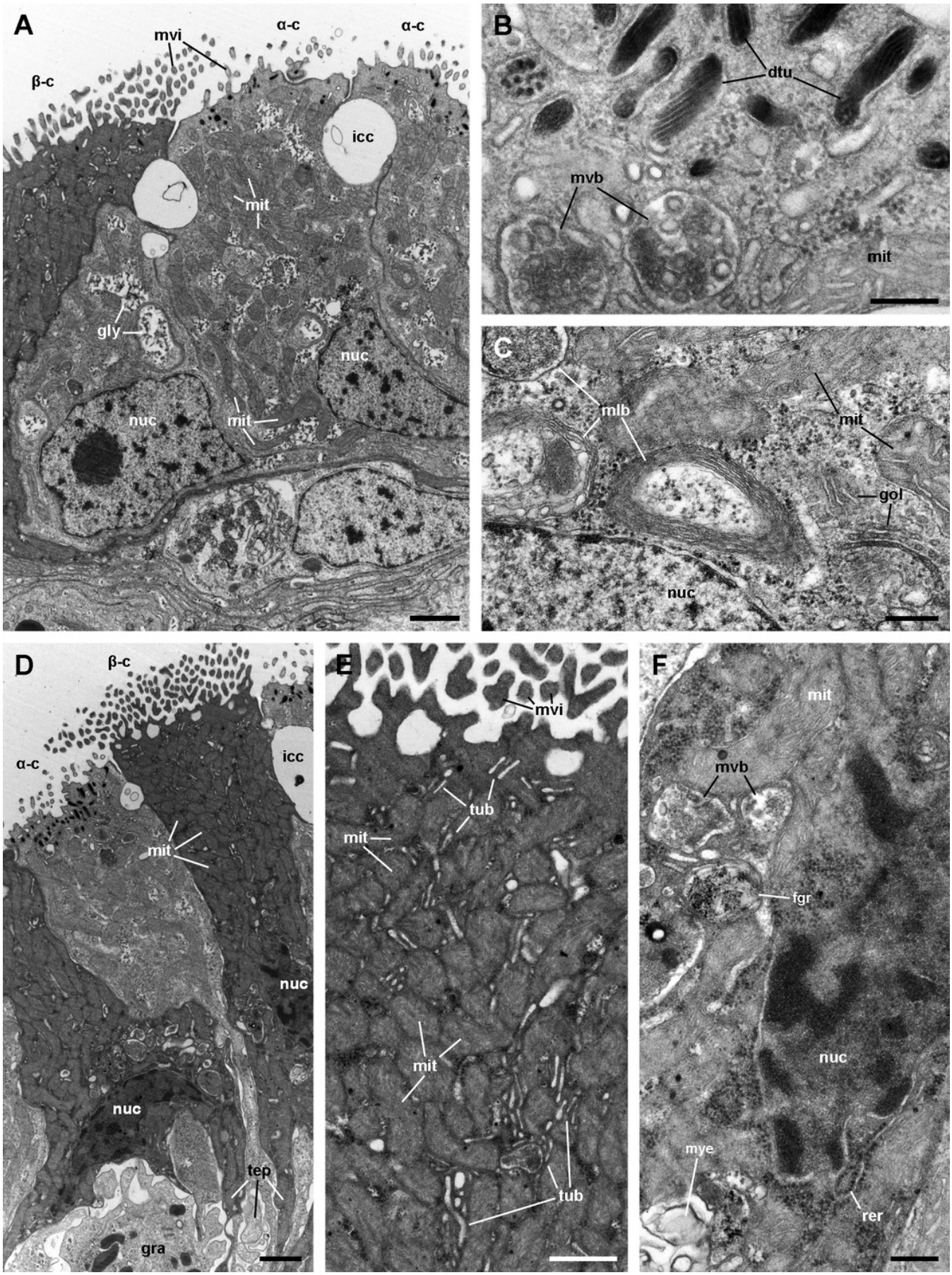
A
mvi
α-c
α-c
β-c
icc
mit
gly
nuc
nuc
mit
B
dtu
mvb
mit
C
mlb
mit
gol
nuc
D
β-c
α-c
icc
mit
nuc
nuc
tep
gra
E
mvi
tub
mit
mit
tub
F
mit
mvb
fgr
nuc
mye
rer

Figure 9

Structures associated with granulocytes in the basolateral domain of the gill epithelium (transmission electron microscopy).

(A) Labyrinth of thin cellular extensions projecting towards the collagen matrix of the underlying connective tissue, where sparse muscle fibres occur. Subepithelial and intraepithelial (arrows) neurite bundles with accompanying glial cells also occur. (B) A granulocyte in close proximity to the basal lamina occupies an enlarged intercellular space. Small intercellular spaces or canaliculi are also seen. (C) Discontinuities in the basal mesh of epithelial projections connect the intercellular spaces directly with the basal lamina, which shows interspersed electron dense thickenings (arrowheads). (D) Basolateral infoldings of an α-cell, adjacent to a β-cell. Scale bars represent: (A–B) 2 µm; (C) 1 µm; (D) 500 nm. Abbreviations: bla, basal lamina; bsi, blood sinus; col, collagen matrix; gra, granulocyte; grn, R granule; icc, intercellular canaliculi; ics, intercellular space; msc, muscle cell; neu, neurite bundle; tep, thin epithelial projections.

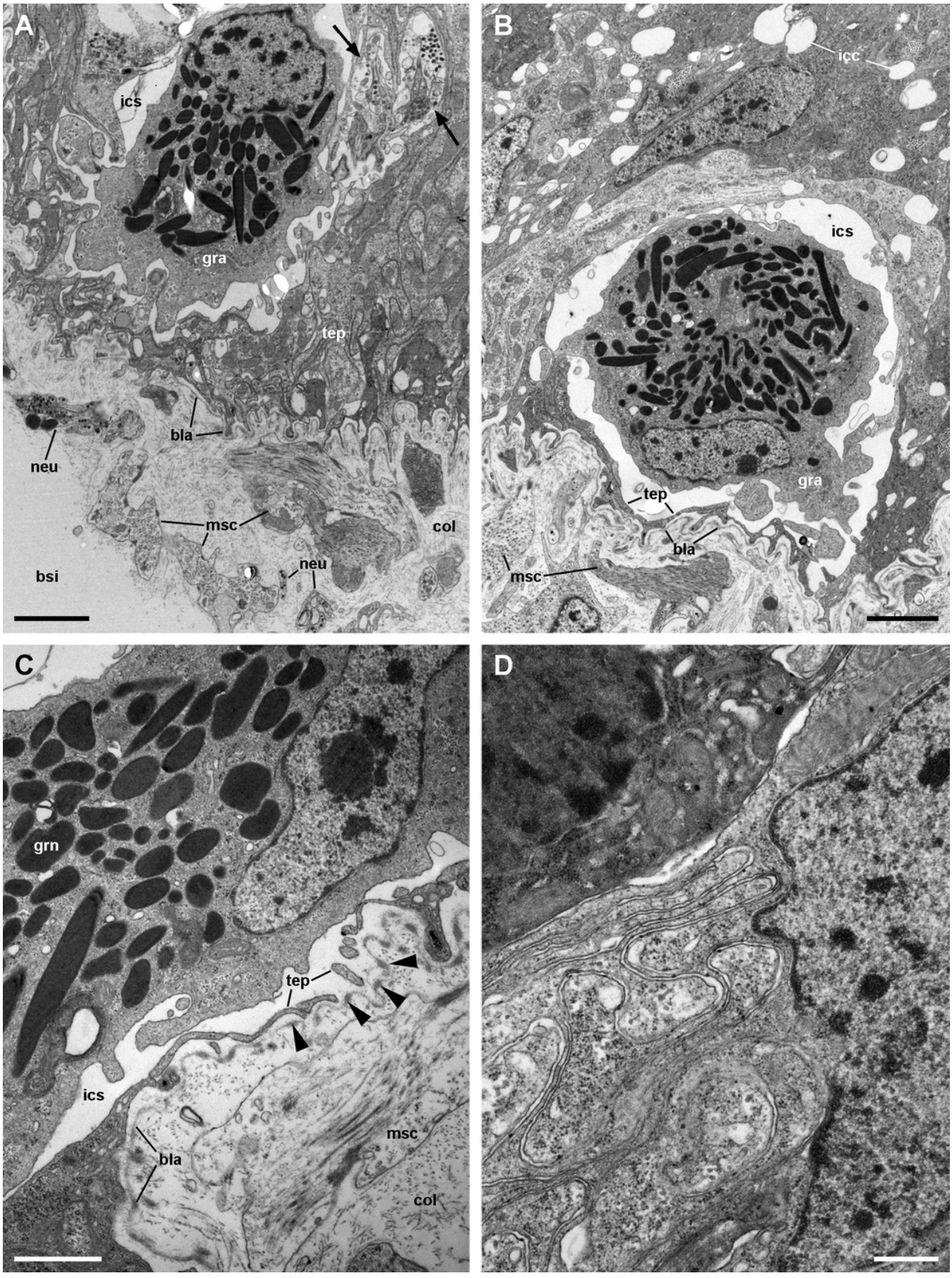
A
ics
gra
tep
bla
neu
msc
col
neu
bsi
B
icc
ics
gra
tep
bla
msc
C
grn
tep
ics
msc
bla
col
D

Figure 10

Long cilia cells (C2) in region III of the gill leaflets (transmission electron microscopy).

(A) Diagram. (B) C2 cells exhibit an electron dense cytoplasm with abundant rough endoplasmic reticulum and glycogen deposits. These cells rest on a thick and electron dense basal lamina (arrowheads). There are extensive intercellular spaces and smaller canaliculi, also seen under light microscopy (Figure 4D). (C) Transverse section of a cilium shows the typical 9+2 microtubule arrangement and membrane blebs (arrows). (D) Membrane-bound bundles of electron-dense tubules/filaments in the apical domain of a C2 cell. Scale bars represent: (B) 1 µm; (C) 50 nm; (D) 250 nm. Abbreviations: adh, adherent junction; bla, basal lamina; cil, cilia; dtu, bundles of electron-dense tubules; gly, glycogen deposit; icc, intercellular canaliculi; ics, intercellular space; msc, muscle cell; mtb, microtubules; mvi, microvilli; neu, neurite bundle; rer, rough endoplasmic reticulum; sep, septate junction; tep, thin epithelial projections.

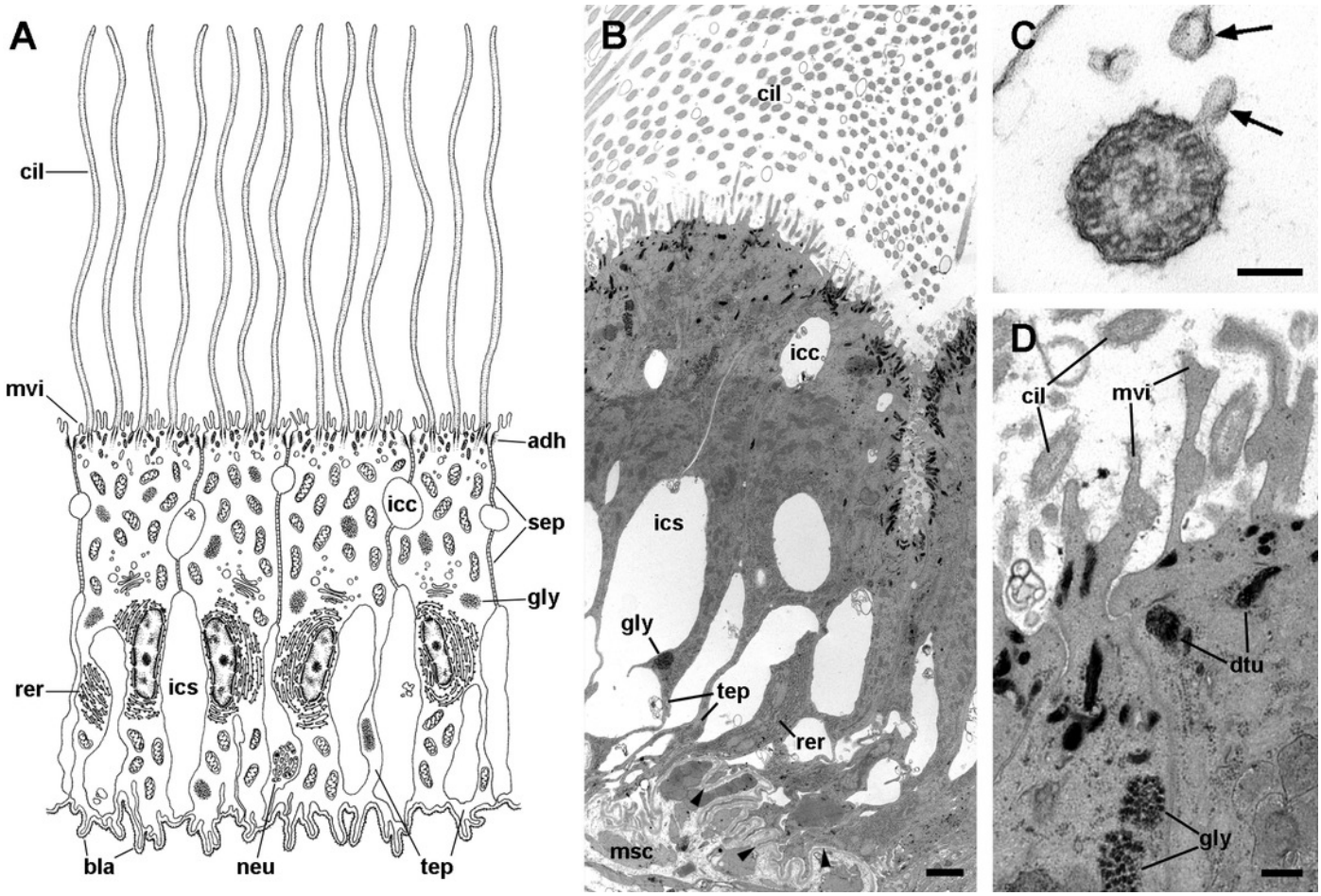
A
cil
mvi
adh
icc
sep
gly
rer
ics
bla
neu
tep
B
cil
icc
ics
gly
tep
rer
msc
C
D
cil
mvi
dtu
gly

Figure 11

Ciliary (C1) and secretory (S1 and S2) cells in region IV of the gill leaflets (transmission electron microscopy).

(A) Diagram. (B) C1 cells exhibit a moderately electron-dense cytoplasm containing large dense-cored granules and a heterochromatic nucleus. Apically, there are finger-like microvilli and short cilia with membrane blebs. Glycogen deposits are also found. (C) An S1 cell showing granules above the nucleus, which contain an inner electron-dense mesh. (D) An S1 cell showing a large accumulation of granules with a looser electron-dense mesh, in the apex. (E) An S2 cell with the cytoplasm almost filled with vacuoles containing a microgranular substance of moderate electron density. Scale bars represent: (B) 1 µm; (C) 500 nm; (D–E) 1 µm. Abbreviations: adh, adherent junction; bla, basal lamina; cil, cilia; dcg, dense-core granules; dtu, bundles of electron-dense tubules; gly, glycogen deposit; icc, intercellular canaliculi; ics, intercellular space; mug, mucinogen granules; mvb, multivesicular body; mvi, microvilli; neu, neurite bundle; nuc, cell nucleus; sep, septate junction; tep, thin epithelial projections; vac, vacuoles.

**Note: Auto Gamma Correction was used for the image. This only affects the reviewing manuscript. See original source image if needed for review.*

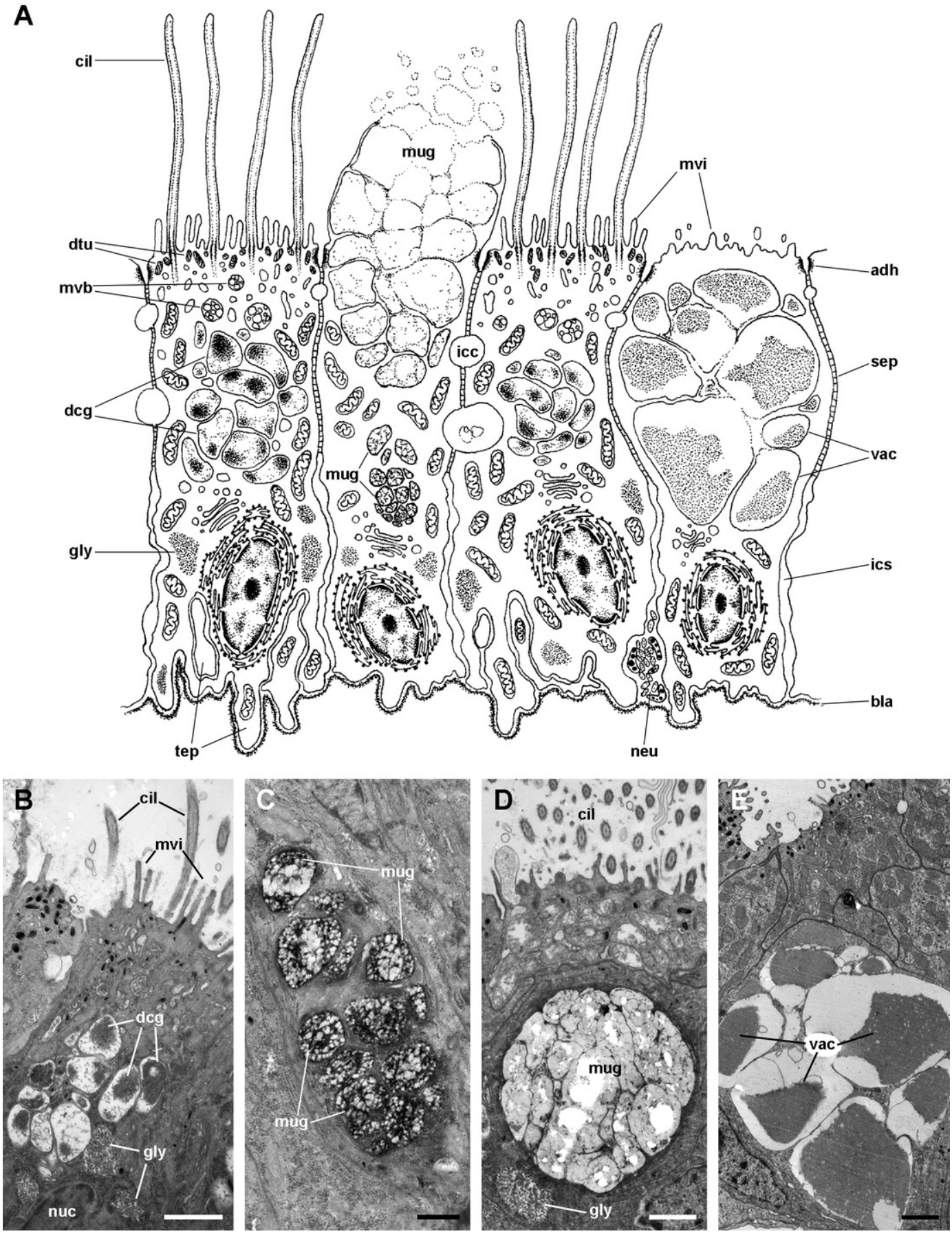
A
cil
mug
mvi
dtu
mvb
adh
icc
sep
dcg
vac
mug
gly
ics
bla
tep
neu
B
cil
mvi
dcg
gly
nuc
C
mug
mug
D
cil
mug
gly
E
vac

Figure 12

Cell junctions in the gill epithelium (transmission electron microscopy).

(A) Apical adherent junction followed by a short septate junction and an intercellular canaliculum with some content. (B) A septate junction. (C) Widening of an intercellular space below the septate junction. Scale bars represent 200 nm. Abbreviations: adh, adherent junction; dtu, bundles of electron-dense tubule; icc, intercellular canaliculi; ics, intercellular space; mit, mitochondrion; sep, septate junction; tub, tubular system.

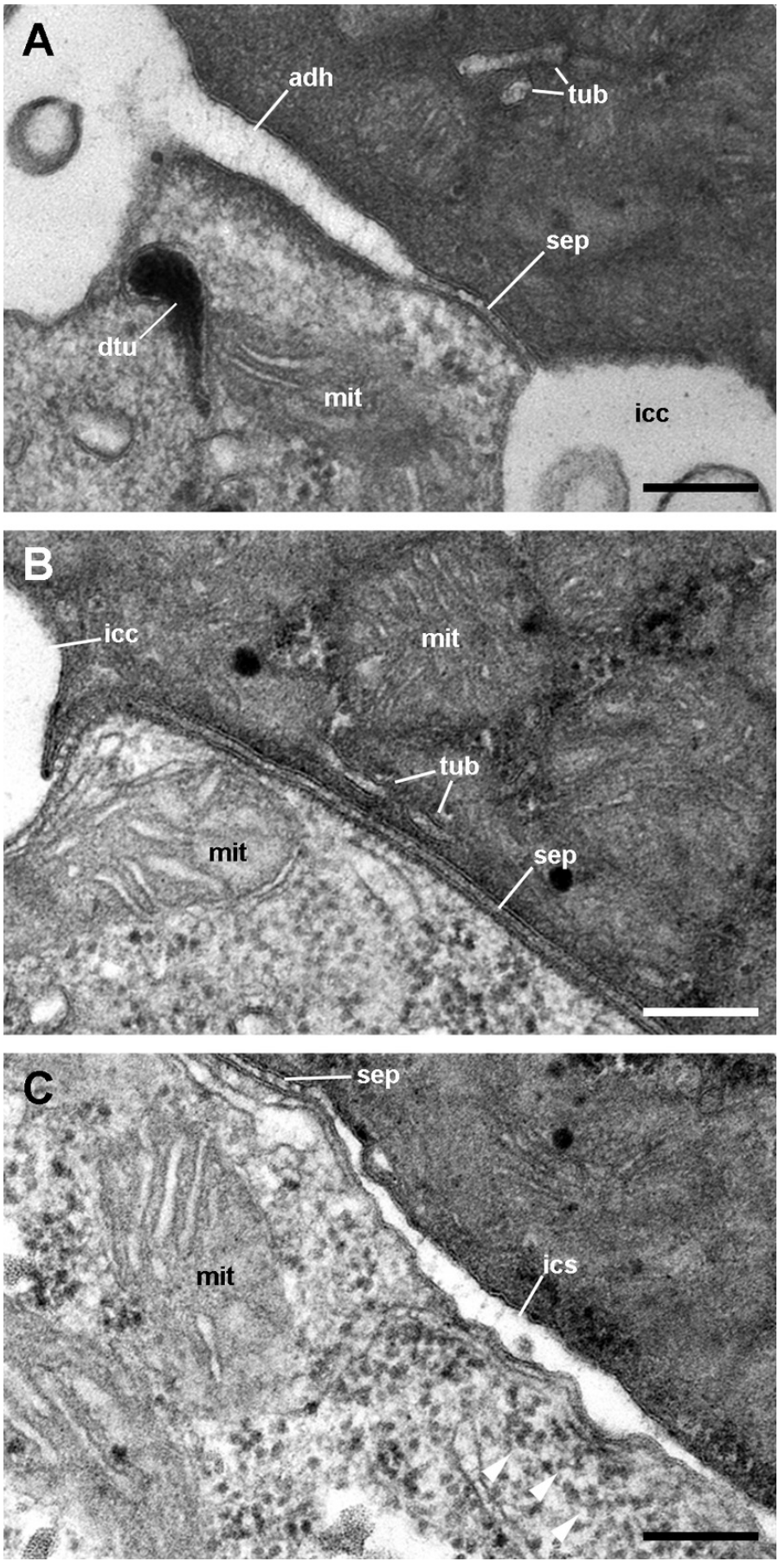
A
adh
tub
sep
dtu
mit
icc
B
icc
mit
tub
mit
sep
C
sep
mit
ics

Figure 13

Fibromuscular tissue and fine innervation of the gill leaflets (transmission electron microscopy).

(A) Overview of the basal domain of epithelial cells, together with a granulocyte in contact with the basal lamina (arrowheads). The underlying tissue exhibits a neurite/glial bundle and trabecular fibromuscular cells with inner myofibrils and electron-dense anchoring junctions with the collagen matrix and the basal lamina. Also notice some intraepithelial neurites (white arrows). (B) Detail of anchoring junctions showing the external brush-like plaque and the internal amorphous electron-dense layer. (C) Detail of a neurite bundle showing neurites associated with glial cells' processes containing granules of different sizes and electron density. Glial cells, or rarely uncovered neurite bundles, are in contact with muscle fibres or trabeculae. Scale bars represent: (A) 1 µm; (B) 500 nm; (C) 500 nm. Abbreviations: anc; anchoring junction; col, collagen matrix; gcp, glial cell process; gra, granulocyte; ics, intercellular space; mit, mitochondria; msc, muscle cells; myo, myofibrils; nee, presumptive nerve endings; neu, neurite bundles; tep, thin epithelial projection.

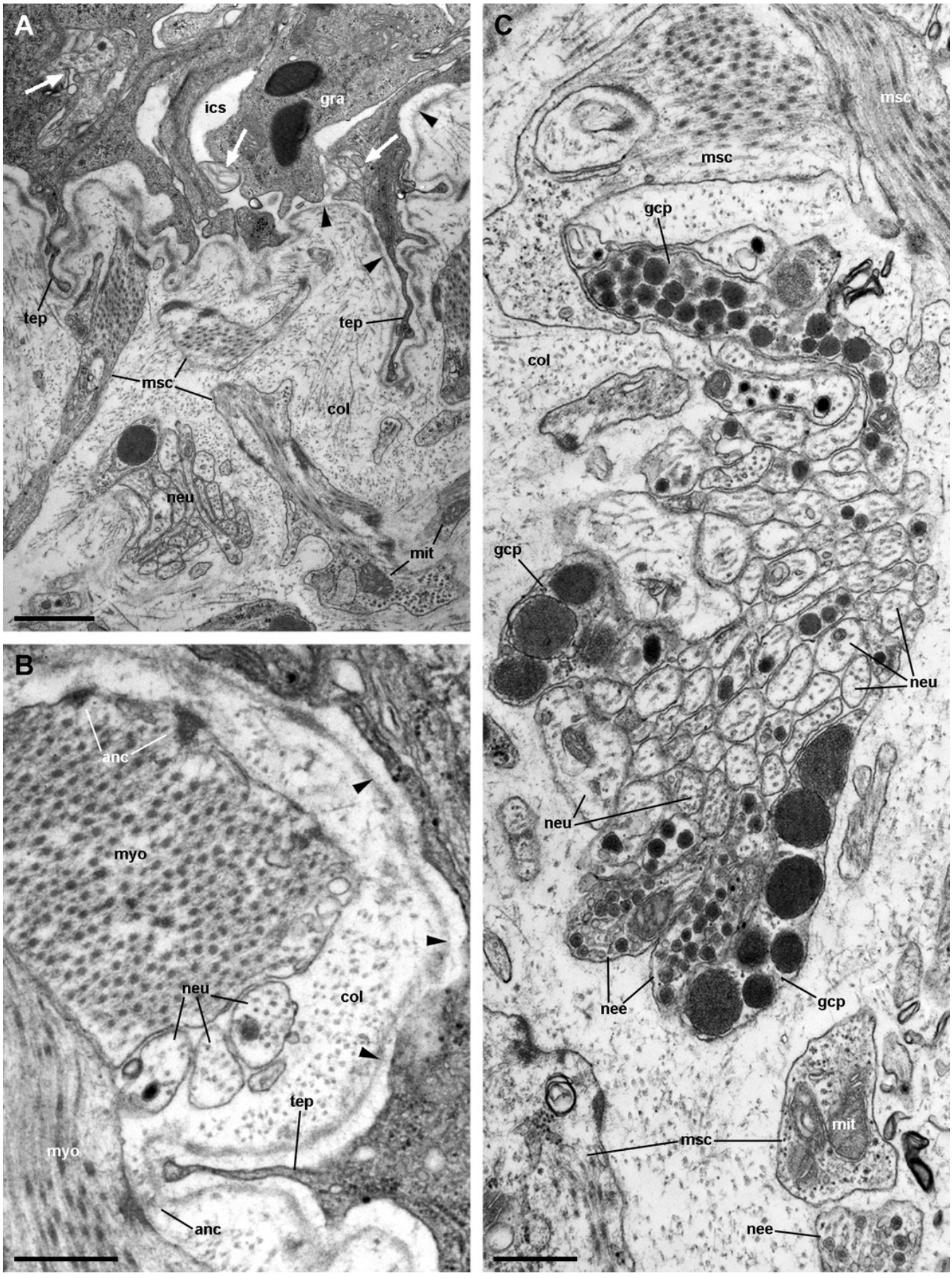
A
ics
gra
tep
tep
msc
col
neu
mit
B
anc
myo
neu
col
tep
myo
anc
C
msc
msc
gcp
col
gcp
neu
neu
nee
gcp
mit
msc
nee

Table 1(on next page)

Cell types and other features of the gill leaflet regions.

1

Region	Epithelial cell types			Epithelial intercellular spaces	Underlying tissues
	Microvillar cells	Ciliary cells	Secretory cells		
I	α and β	C1	S1 and S2 (scarce)	Extensive spaces, with numerous granulocytes	Thin basal lamina Loose fibromuscular tissue Thin trabeculae cross the laminar leaflet sinus
II	α	None	S1 and S2 (abundant)	Narrow spaces, scarce granulocytes	Thick basal lamina Dense fibromuscular tissue Thin trabeculae cross the marginal leaflet sinus
III	None	C2	None	Extensive spaces, scarce granulocytes	Thick basal lamina Dense fibromuscular tissue Thick trabeculae cross the marginal leaflet sinus
IV	α	C1	Abundant S1 and S2	Narrow spaces, scarce granulocytes	Thick basal lamina Skeletal rod Leaflet nerve

2 Abbreviations: α, α-cells; β, β-cells; C1, short cilia cells; C2, long cilia cells; S1, metachromatic secretory
3 cells; S2, orthochromatic secretory cells.

Table 2(on next page)

Features of the cell types in the gill epithelium of *P. canaliculata*.

Cell type	Apical specialisations	Nucleus and cytoplasm	Endomembrane system	Other membrane-bound bodies
α	Few and short, finger-like microvilli	Euchromatic nucleus Abundant, long mitochondria	Abundant RER Golgi bodies Vesicular system Multivesicular bodies Multilamellar bodies	Bundles of electron-dense tubules/filaments Dense-cored granules (in region IV only)
β	Numerous and long, ramified microvilli	Heterochromatic nucleus Tightly-packed, short mitochondria	Tubular system Multivesicular bodies Myeloid and fibrogranular bodies	Few and small bundles of electron-dense tubules/filaments
C1	Short cilia with membrane blebs Short, finger-like microvilli	Heterochromatic nucleus Rather dark cytoplasm	Vesicular system Multivesicular bodies	Abundant and large dense-cored granules Bundles of electron-dense tubules/filaments
C2	Very long cilia with membrane blebs Short, finger-like microvilli	Euchromatic nucleus Rather dark cytoplasm	Abundant RER	Bundles of electron-dense tubules/filaments
S1	None	Heterochromatic nucleus Rather dark cytoplasm	Abundant RER Golgi bodies	Mucinogen granules (basally, with an electron-dense mesh; apically, with a looser electron-dense mesh)
S2	None	Euchromatic nucleus Clear cytoplasm	Abundant RER Golgi bodies	Granules with moderately electron-dense cores
G	–	Euchromatic nucleus Clear cytoplasm	Golgi bodies	R granules

Abbreviations: α, α-cells; β, β-cells; C1, short cilia cells; C2, long cilia cells; S1, metachromatic secretory cells; S2, orthochromatic secretory cells; G, granulocytes; RER, rough endoplasmic reticulum.